USGS
science for a changing world

U.S. Department of the Interior
U.S. Geological Survey

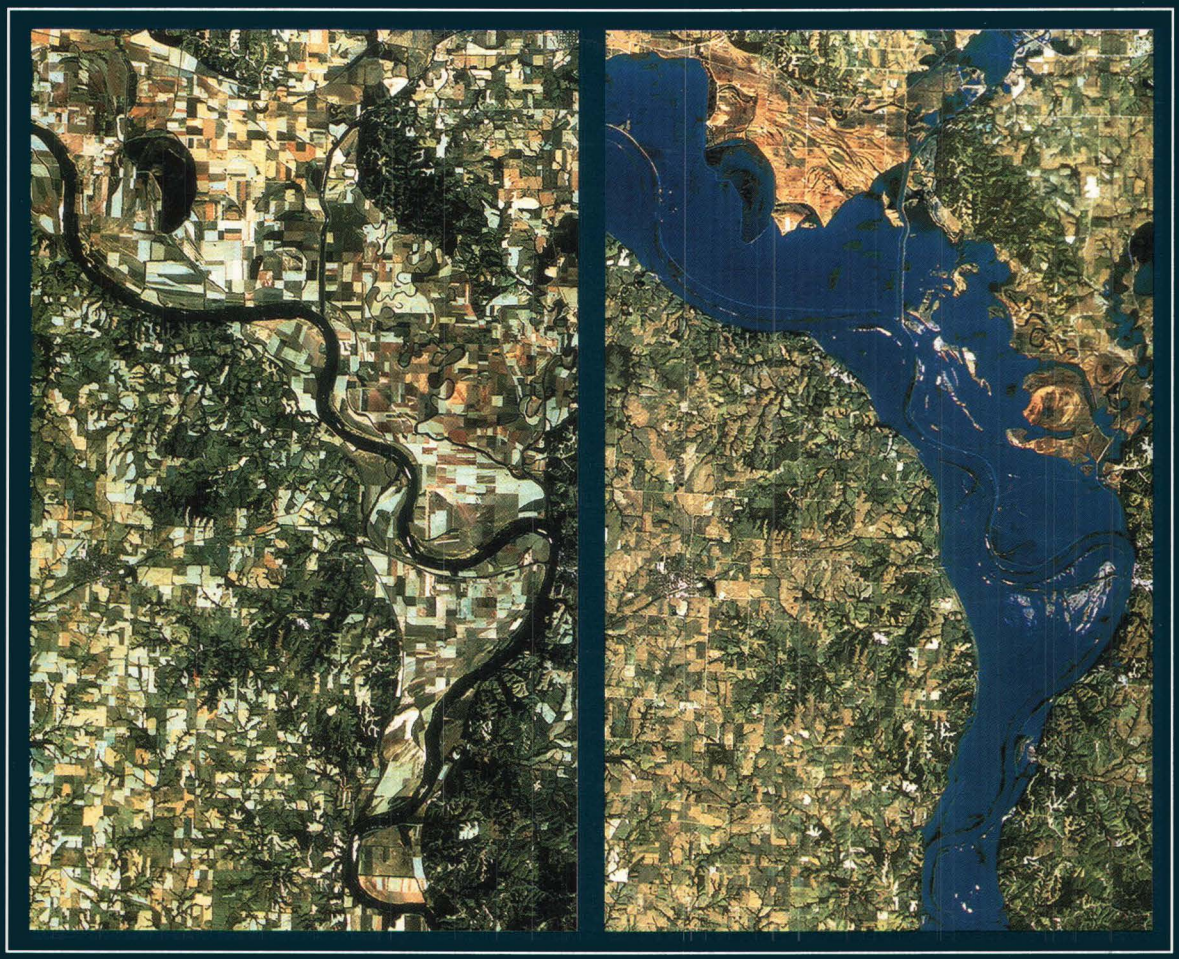

Historical Landsat Data Comparisons

Illustrations of the Earth's Changing Surface

Historical Landsat Data Comparisons

Illustrations of the Earth's Changing Surface

March 1995

U.S. Department of the Interior
U.S. Geological Survey
EROS Data Center

Table of Contents

Introduction

The U.S. Geological Survey's (USGS) EROS Data Center (EDC) has managed the Landsat data archive for more than two decades. This archive provides a rich collection of information about the Earth's land surface. Major changes to the surface of the planet can be detected, measured, and analyzed using Landsat data. The effects of desertification, deforestation, pollution, cataclysmic volcanic activity, and other natural and anthropogenic events can be examined using data acquired from the Landsat series of Earth-observing satellites. The information obtainable from the historical and current Landsat data play a key role in studying surface changes through time.

This document provides an overview of the Landsat program and illustrates the application of the data to monitor changes occurring on the surface of the Earth. To reveal changes that have taken place within the past 20 years, pairs and triplicates of images were constructed from the Landsat multispectral scanner (MSS) and thematic mapper (TM) sensors. Landsat MSS data provide a historical record of the Earth's land surface from the early 1970's to the early 1990's. Landsat TM data provide land surface information from the early 1980's to the present.

A Brief History of the Landsat Program

The concept of a civilian Earth resources satellite was conceived in the Department of Interior in the mid-1960's. The National Aeronautics and Space Administration (NASA) embarked on an initiative to develop and launch the first Earth monitoring satellite to meet the needs of resource managers and Earth scientists. The USGS entered into a partnership with NASA in the early 1970's to assume responsibility for data archiving and distribution of data products. On July 23, 1972, NASA launched the first in a series of satellites designed to provide repetitive global coverage of the Earth's land masses. Designated initially as the Earth Resources Technology Satellite-A (ERTS-A), it used a Nimbus-type platform that was modified to carry sensor systems and data relay equipment. When operational orbit was achieved, it was designated ERTS-1.

The satellite continued to function beyond its designed life expectancy of 1 year and finally ceased to operate on January 6, 1978, more than 5 years after its launch date. The second in this series of Earth resources satellites (designated ERTS-B) was launched January 22, 1975. It was renamed Landsat 2 by NASA, which also renamed ERTS-1 to Landsat 1. Three additional Landsats were launched in 1978, 1982, and 1984 (Landsats 3, 4, and 5 respectively). Each successive satellite system had improved sensor and communications capabilities (table 1).

NASA was responsible for operating the Landsats through the early 1980's. In January 1983, operations of the Landsat system were transferred to the National Oceanic and Atmospheric Administration (NOAA). In October 1985, the Landsat system was commercialized and the Earth Observation Satellite Company assumed responsibility for its operation. Throughout these changes, the EDC retained primary responsibility as the Government archive of Landsat data. The Land Remote Sensing Policy Act of 1992 (Public Law 102-555) officially authorized the National Satellite Land Remote Sensing Data Archive and assigned responsibility to the Department of the Interior. In addition to its Landsat data management responsibility the EDC investigates new methods of characterizing and studying changes on the land surface with Landsat data.

Table 1

Background information and status of Landsat satellites.

Satellite	Launched	Decommissioned	Sensors
Landsat 1	July 23, 1972	January 6, 1978	MSS and RBV
Landsat 2	January 22, 1975	February 25, 1982	MSS and RBV
Landsat 3	March 5, 1978	March 31, 1983	MSS and RBV
Landsat 4	July 16, 1982	*	TM and MSS
Landsat 5	March 1, 1984	**	TM and MSS
Landsat 6	October 5, 1993	***	ETM
Landsat 7	Fall 1998****		ETM +*****

* in standby mode
** operational
*** never achieved orbit
**** anticipated launch
***** The sensor onboard Landsat 6 was called the enhanced thematic mapper (ETM). Landsat 7 will carry the enhanced thematic mapper plus (ETM+).

Characteristics of the Landsat System

Landsats 1 through 3 operated in a near-polar orbit at an altitude of 920 km with an 18-day repeat coverage cycle. These satellites circled the Earth every 103 minutes, completing 14 orbits a day (fig. 1). Eighteen days and 251 overlapping orbits were required to provide nearly complete coverage of the Earth's surface with 185 km wide image swaths. The amount of swath overlap or sidelap varies from 14 percent at the Equator to a maximum of approximately 85 percent at 81° north or south latitude (fig. 2). These satellites carried two sensors: a return beam vidicon (RBV) and a MSS. The RBV sensor was essentially a television camera and did not achieve the popularity of the MSS sensor. The MSS sensor scanned the Earth's surface from west to east as the satellite moved in its descending (north-to-south) orbit over the sunlit side of the Earth. Six detectors for each spectral band provided six scan lines on each active scan. The combination of scanning geometry, satellite orbit, and Earth rotation produced the global coverage necessary for studying land surface change (fig. 3). The resolution of the MSS sensor was approximately 80 m with radiometric coverage in four spectral bands from the visible green to the near-infrared (IR) wavelengths (table 2). Only the MSS sensor on Landsat 3 had a fifth band in the thermal-IR.

Landsats 4 and 5 carry both the MSS and the TM sensors; however, routine collection of MSS data was terminated in late 1992. They orbit at an altitude of 705 km and provide a 16-day, 233-orbit cycle with a swath overlap that varies from 7 percent at the Equator to nearly 84 percent at 81° north or south latitude. These satellites were also designed and operated to collect data over a 185 km swath. The MSS sensors aboard Landsats 4 and 5 are identical to the ones that were carried on Landsats 1 and 2. The MSS and TM sensors primarily detect reflected radiation from the Earth in the visible and IR wavelengths, but the TM sensor provides more radiometric information than the MSS sensor. The wavelength range for the TM sensor is from the visible (blue), through the mid-IR, into the thermal-IR portion of the electromagnetic spectrum (table 3). Sixteen detectors for the visible and mid-IR wavelength bands in the TM sensor provide 16 scan lines on each active scan. Four detectors for the thermal-IR band provide four scan lines on each active scan. The TM sensor has a spatial resolution of 30 m for the visible, near-IR, and mid-IR wavelengths and a spatial resolution of 120 m for the thermal-IR band.

All of the Landsats have been in sun-synchronous orbits with equatorial crossing times ranging from 8:30 a.m. for Landsat 1 to 9 a.m. for Landsat 2 to the current time of 9:45

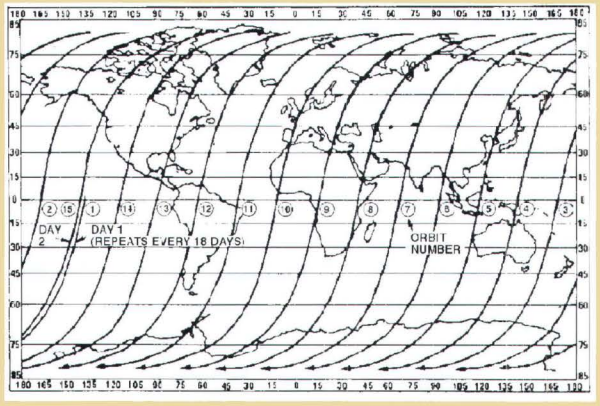

Figure 1. Typical daily orbit pattern for Landsats 1 through 3 (from Landsat Data Users Handbook, 1979, USGS).

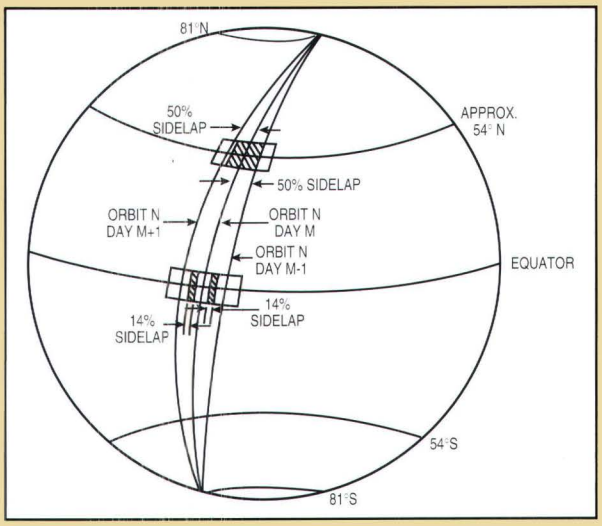

Figure 2. Poleward increase of sidelap between adjacent tracks of Landsats 1 through 3 (from Landsat Data Users Handbook, 1979, USGS).

a.m. for Landsat 5, and the proposed time of 10 a.m. for Landsat 7.

Characteristics of Landsat Data

Since 1972 these satellites have provided repetitive, synoptic, global coverage of high-resolution multispectral imagery. The characteristics of the MSS and TM bands were selected to maximize their capabilities for detecting and monitoring different types of Earth's resources. For example, MSS band 1 (band 2 of TM) can detect green reflectance from healthy vegetation, and band 2 of MSS (band 3 of TM) is designed for detecting chlorophyll absorption in vegetation. MSS bands 3 and 4 (TM band 4) are ideal for near-IR reflectance peaks in healthy green vegetation and for detecting water-land interfaces. TM band 1 can penetrate water for bathymetric mapping along coastal areas and is useful for soil-vegetation differentiation and for distinguishing forest types. The two mid-IR red bands on TM (bands 5 and 7) are useful for vegetation and soil moisture studies, and discriminating between rock and mineral types. The thermal-IR band on TM (band 6) is designed to assist in thermal mapping, and for soil moisture and vegetation studies.

The Landsat images in this publication are color composite images created by assigning colors to bands. Typically, MSS Bands 4, 2, and 1 can be combined to make false-color composite images where band 4 represents red, band 2, green, and band 1, blue. This band combination makes vegetation appear as shades of red, brighter reds indicating more vigorously growing vegetation. Soils with no or sparse vegetation will range from white (sands) to greens or browns depending on moisture and organic matter content. Water bodies will appear blue. Deep, clear water will be dark blue to black in color, while sediment-laden or shallow waters will appear lighter in color. Urban areas will appear blue-gray in color. Clouds and snow will be bright white. They are usually distinguishable from each other by the shadows associated with

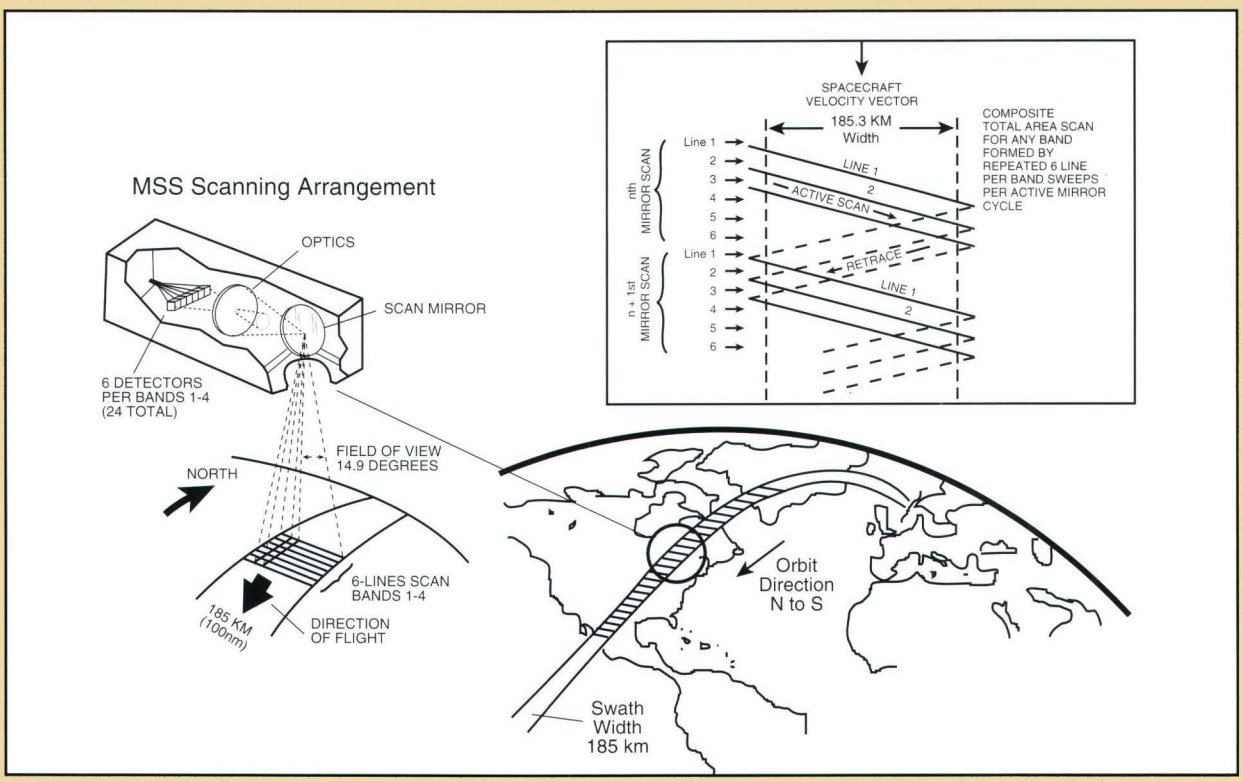

Figure 3. Scanning geometry of the multispectral scanner (from Landsat 4 Data Users Handbook, 1984, USGS).

the clouds. False-color composites can be created with TM data using bands 4, 3, and 2 in red, green, and blue, respectively. The images in this document include examples of both MSS and TM data.

Applications of Landsat Data

Landsat data have been used by government, commercial, industrial, civilian, and educational communities in the U.S. and worldwide. They are being used to support a wide range of applications in such areas as global change research, agriculture, forestry, geology, resources management, geography, mapping, water quality, and oceanography. The Landsat data in this booklet illustrate some of the dramatic changes that have taken place on the Earth in the past 20 years and demonstrate potential applications for monitoring the conditions of the Earth's land surface. The images provide examples of anthropogenic and natural changes on the Earth over periods of several months to more than 15 years. The changes include agricultural development, deforestation, natural disasters, urbanization, and the development and degradation of water resources. The inclination of the orbit has not been corrected in these images, which means each image is oriented about 10 degrees east of north. The locator map on the following pages provides a quick geographic reference to the images. These images represent a small proportion of the Landsat data archive at the EDC. The MSS archive has over 600,000 scenes with a data volume of 20 terabytes. The TM archive has over 300,000 scenes with a data volume of over 50 terabytes.

Table 2

Radiometric range of bands and resolution for the MSS sensor (from Landsat Data Users Handbook, 1979 and 1984, USGS).

Landsats 1-3	Landsats 4-5	Wavelength (micrometers)	Resolution (meters)
Band 4	Band 1	0.5 - 0.6	79/82*
Band 5	Band 2	0.6 - 0.7	79/82
Band 6	Band 3	0.7 - 0.8	79/82
Band 7	Band 4	0.8 - 1.1	79/82
Band 8**		10.4 - 12.6	237

* The nominal altitude was changed from 920 km for Landsats 1 to 3 to 705 km for Landsats 4 and 5 which resulted in a resolution of approximately 79 and 82 meters respectively.

** Landsat 3 only.

Table 3

Radiometric range of bands and resolution for the TM sensor (from Landsat 4 Data Users Handbook, 1984, USGS).

Landsats 4-5	Wavelength (micrometers)	Resolution (meters)
Band 1	0.45-0.52	30
Band 2	0.52-0.60	30
Band 3	0.63-0.69	30
Band 4	0.76-0.90	30
Band 5	1.55-1.75	30
Band 6	10.40-12.50	120
Band 7	2.08-2.35	30

About the Cover

Upper Mississippi River Basin Flood of 1993

A series of heavy summer rains, following an unusually wet period from the summer and fall of 1992 through the spring of 1993, caused severe flooding along the Mississippi and Missouri rivers during the summer of 1993. The Landsat TM image on the left shows the Missouri River near Glasgow, Missouri (right side of the image). This image, acquired on September 24, 1992, prior to the floods, shows the extensive agricultural activities in the floodplain and a large oxbow lake (in the upper left of the image).

The TM image on the right was acquired on September 27, 1993, near the maximum flood peak. The flooding below Glasgow extends from bluff to bluff. The flooding upriver has inundated the agricultural fields and the oxbow lake. Terraces above the oxbow lake, predominately light brown and tan, were not flooded during this period.

Locator Map

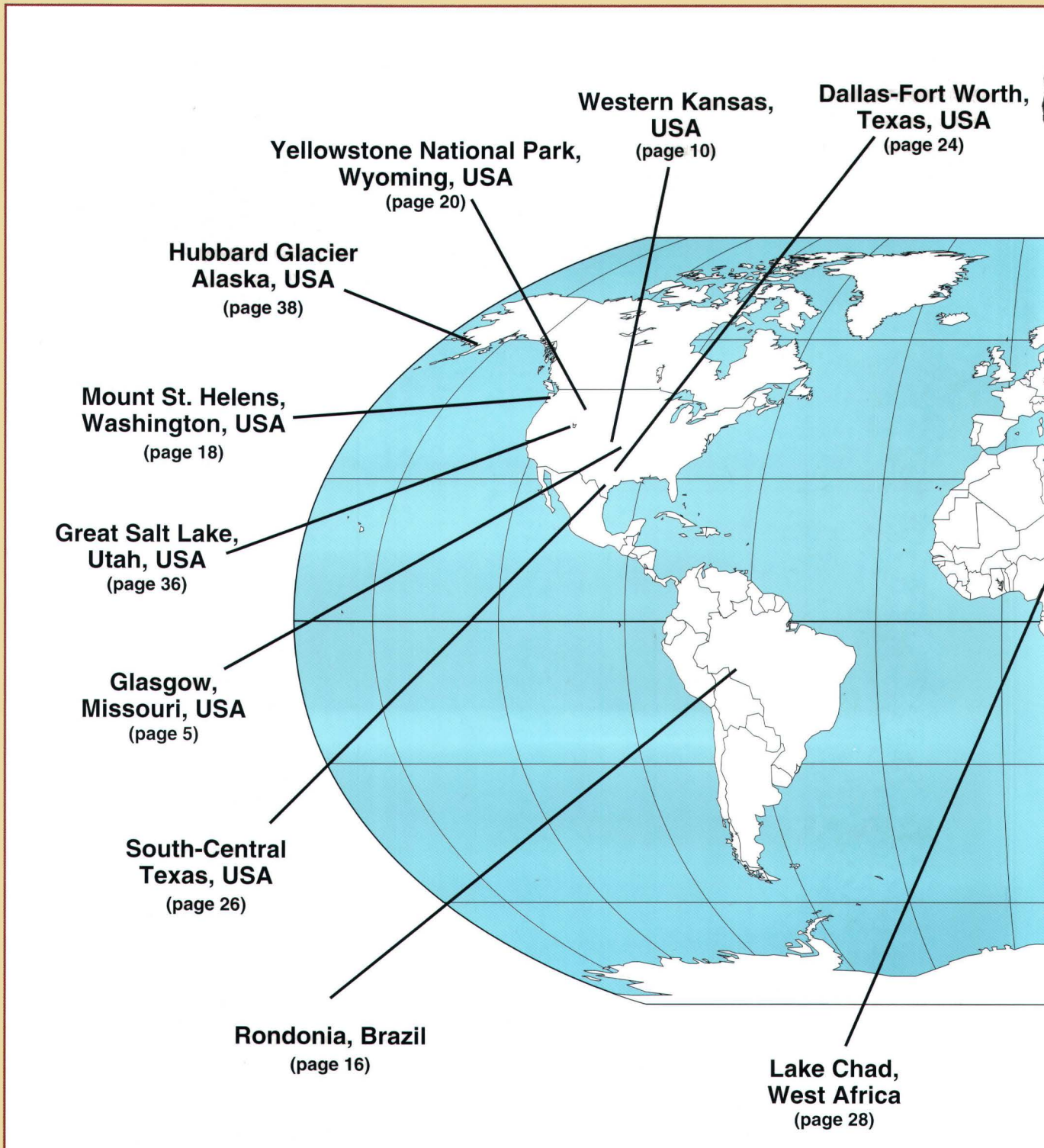
Western Kansas, USA (page 10)
Dallas-Fort Worth, Texas, USA (page 24)
Yellowstone National Park, Wyoming, USA (page 20)
Hubbard Glacier Alaska, USA (page 38)
Mount St. Helens, Washington, USA (page 18)
Great Salt Lake, Utah, USA (page 36)
Glasgow, Missouri, USA (page 5)
South-Central Texas, USA (page 26)
Rondonia, Brazil (page 16)
Lake Chad, West Africa (page 28)

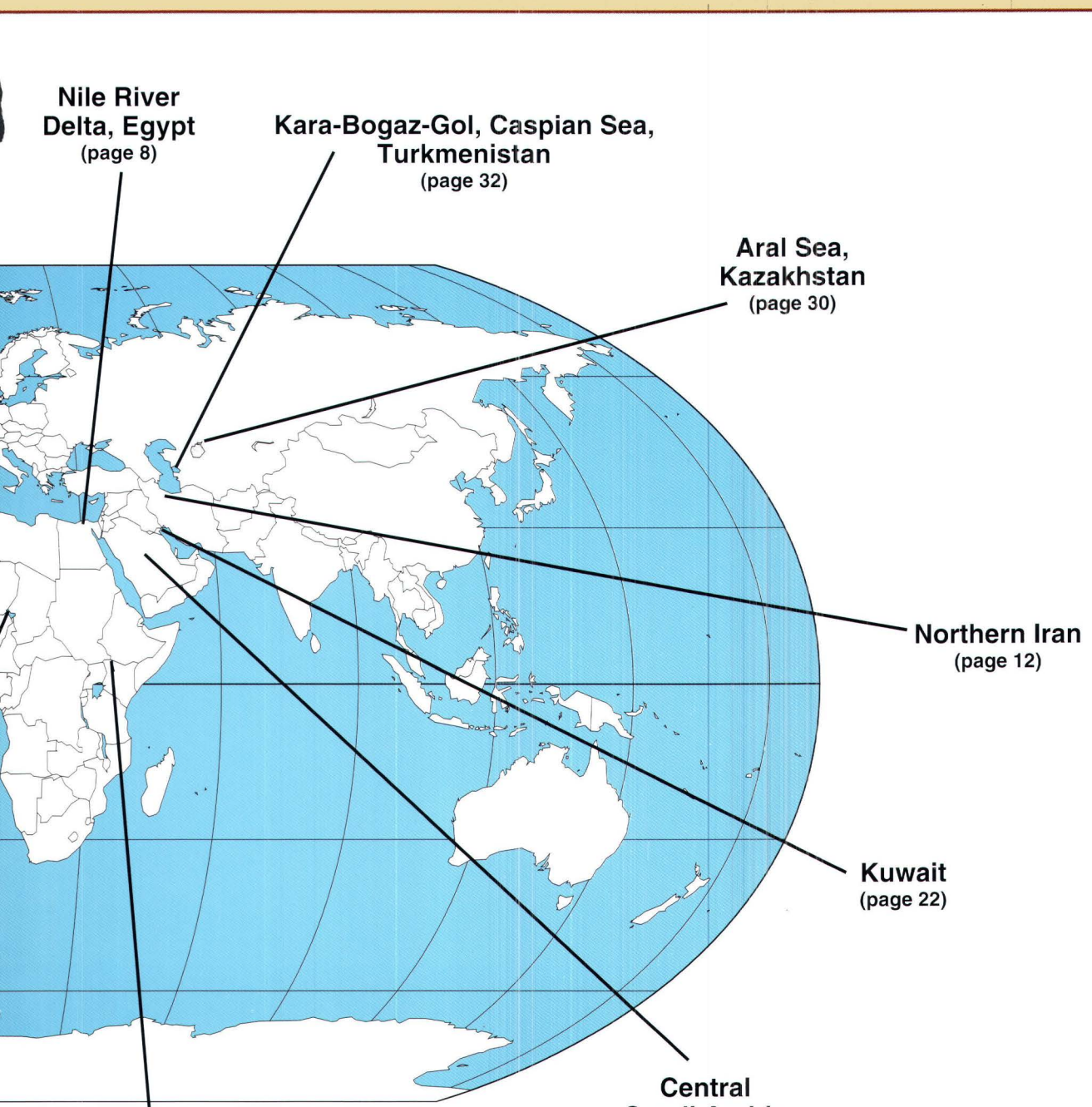
Nile River Delta, Egypt
(page 8)
Kara-Bogaz-Gol, Caspian Sea, Turkmenistan
(page 32)
Aral Sea, Kazakhstan
(page 30)
Northern Iran
(page 12)
Kuwait
(page 22)
Central Saudi Arabia
(page 14)
Lake Turkana, Kenya
(page 34)

Agricultural Development
Urban Growth

Nile River Delta, Egypt

0 10 20 30 40

Scale 1 cm = 9.5 km.

Landsat MSS
May 10, 1973

Images from May 10, 1973, and July 18, 1987, show the dramatic urban growth within the Nile River delta and the expansion of agriculture into adjoining desert areas. Cairo, Egypt, shown as the large blue-gray expanse in the right-central portion of each image, increased in population from 1.5 million in 1947 to 6 million in 1986. It now has a population density of more than 26,000 people per square

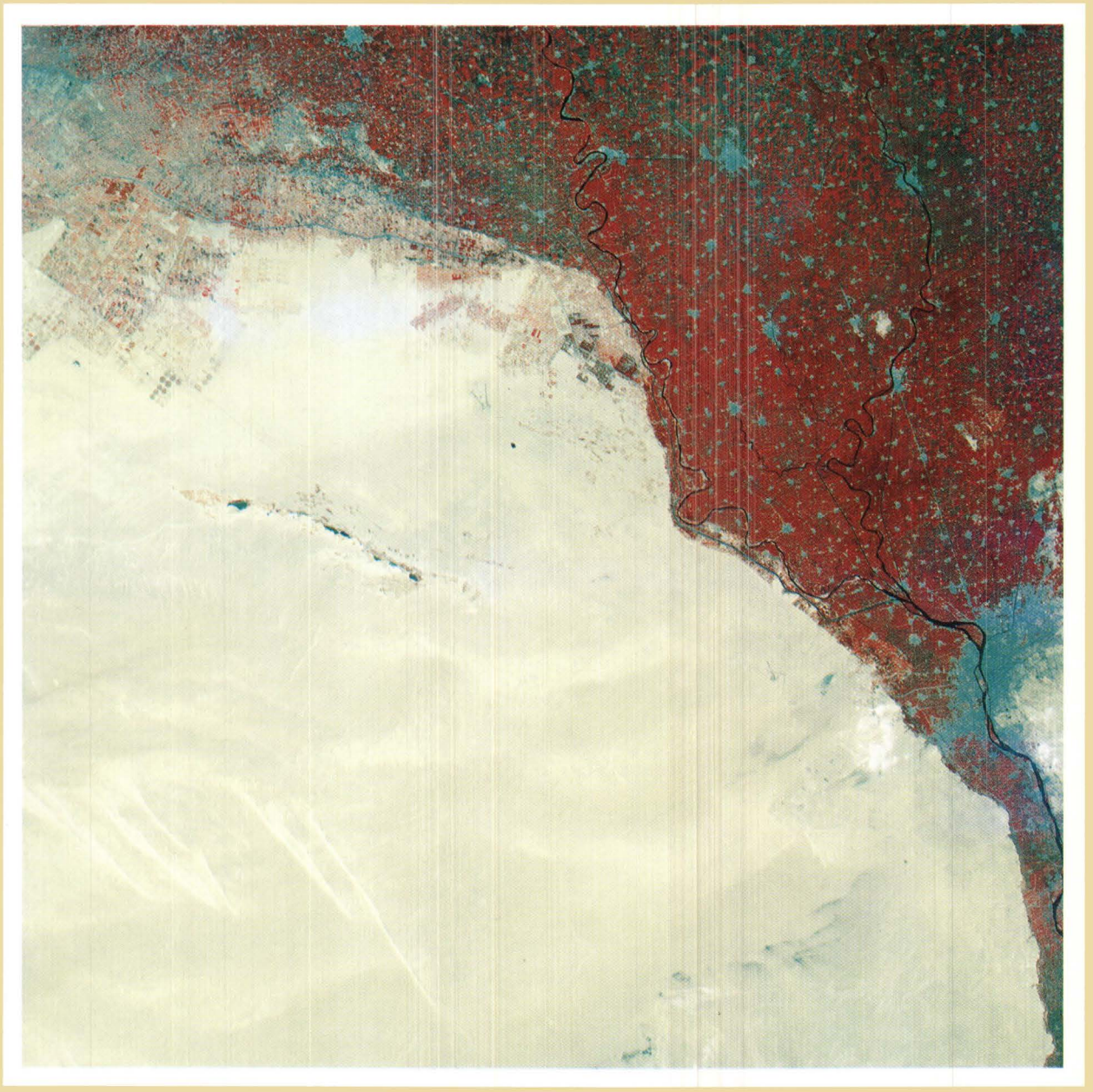

kilometer or more than 11 million people. Urban expansion is also noticeable in the other parts of the delta by the increase in the blue-gray areas in the 1987 image. The area of vegetation just outside the delta in the upper-left area of each image is new agricultural development. Some of the crops in this area are irrigated using center-pivot irrigation. Areas under this type of irrigation appear as red circles.

0 10 20 30 40

Scale 1 cm = 9.5 km.

Landsat MSS
July 18, 1987

Western Kansas, USA

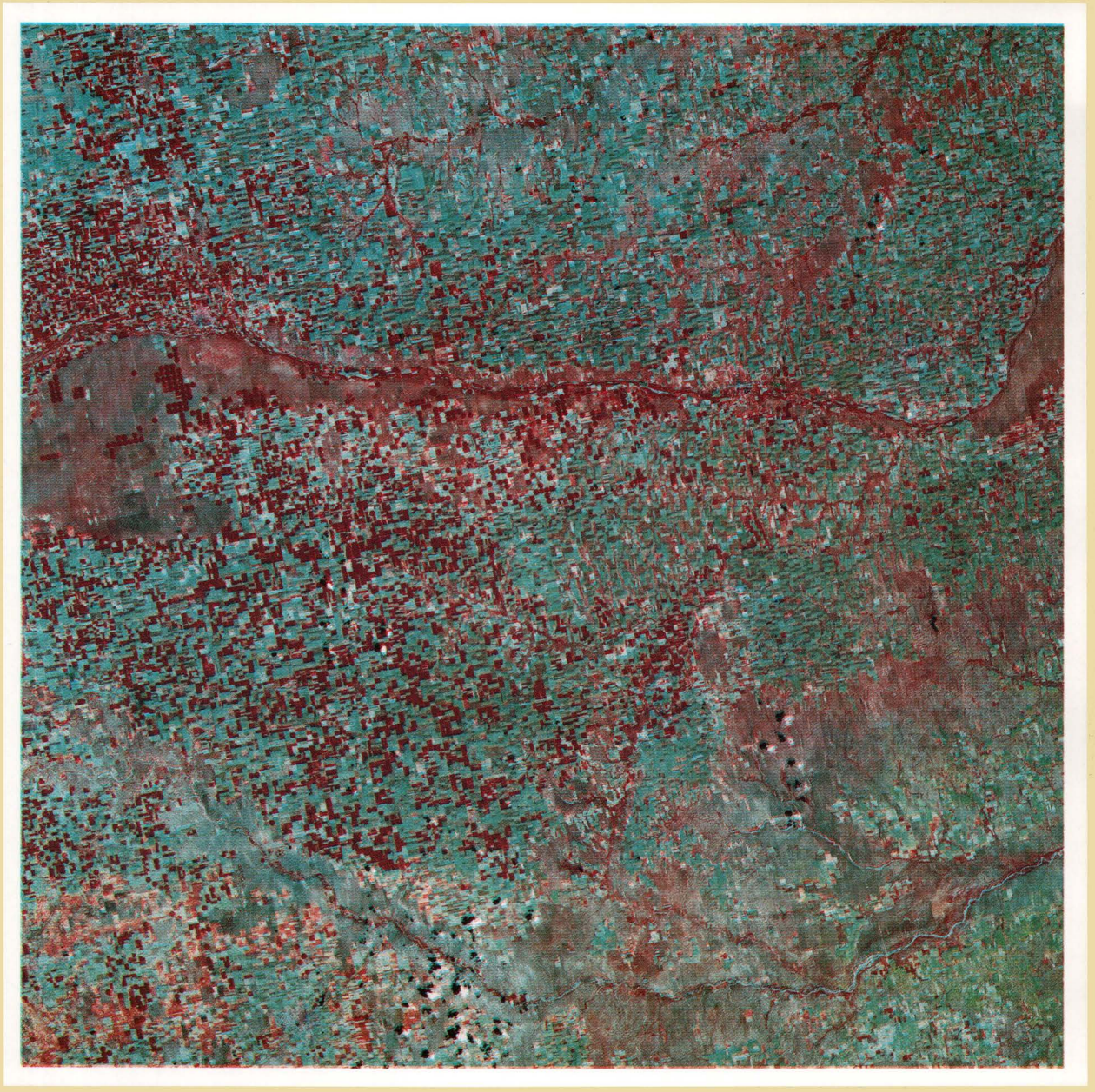

0 10 20 30 40

Scale 1 cm = 9.5 km

Landsat MSS
August 16, 1972

Much of the natural shortgrass prairie of western Kansas is now irrigated cropland. The number of center-pivot irrigation systems in Finney County and adjacent areas of western Kansas has increased dramatically since the early 1970's. Irrigation is possible because of the water available from the Ogallala aquifer, which underlies an area from Nebraska and Wyoming south to the Texas Panhandle. These two August

images show center-pivot irrigated crops as red circles. The predominant crop in this area of Kansas is corn. Light-colored cultivated fields in the images are fallow or recently harvested wheat fields. Images such as these play a major role in providing an inventory of irrigated crop acreage, a key component of modeling aquifer response to changes in water use.

0 10 20 30 40

Scale 1 cm = 9.5 km

Landsat MSS
August 15, 1988

Northern Iran

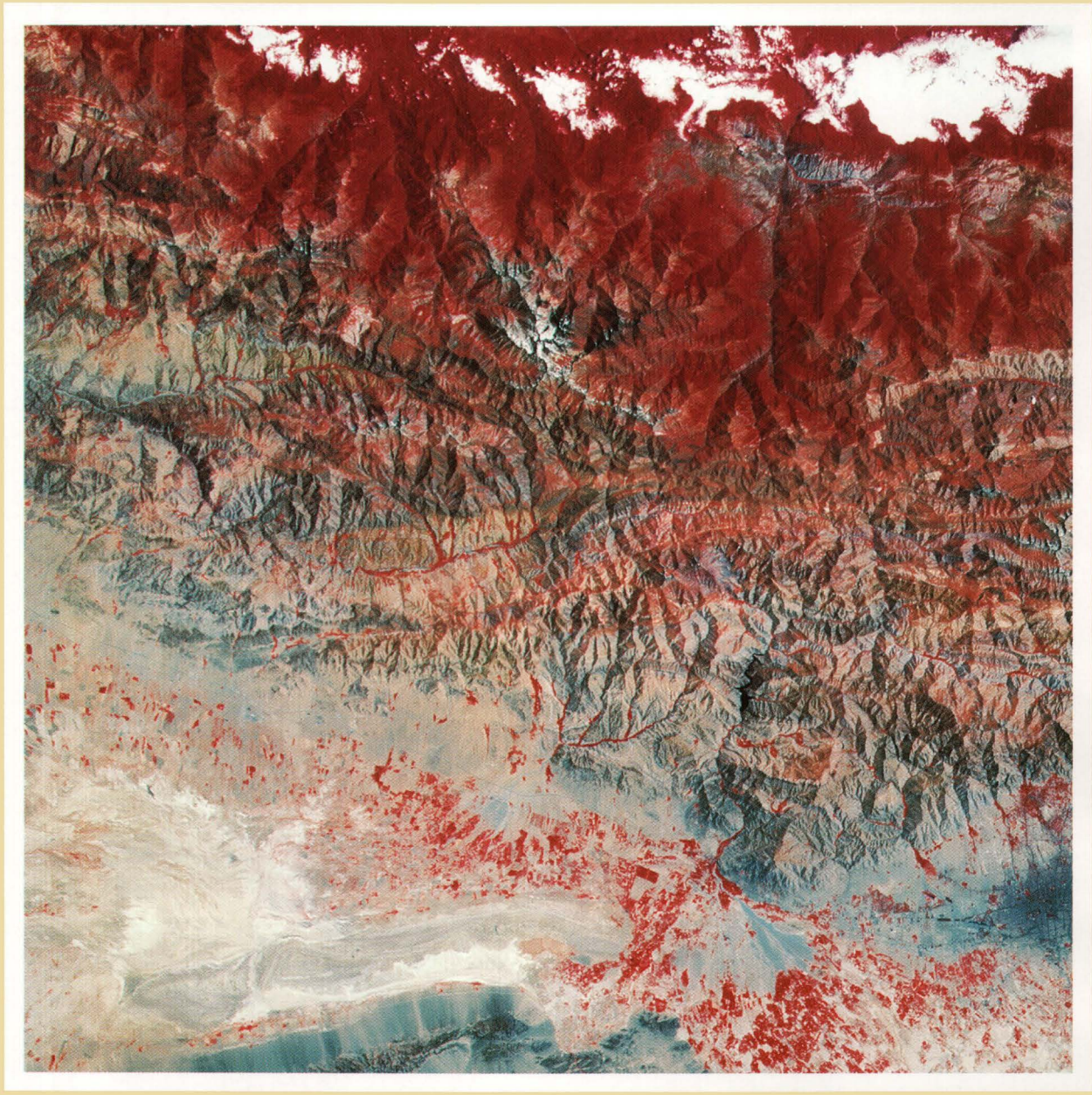

0 10 20 30

Scale 1 cm = 7.6 km

Landsat MSS
July 14, 1977

Irrigated agriculture, shown by the red tones of the field patterns, has increased in the valley (central part of each image) south of the Elburz Mountains in northern Iran, as depicted by these July 14, 1977, and September 16, 1987, images. These mountains run parallel to the Caspian Sea and act as a barrier to rain clouds moving southward. As the rain clouds rise in altitude to cross the mountains, they drop their

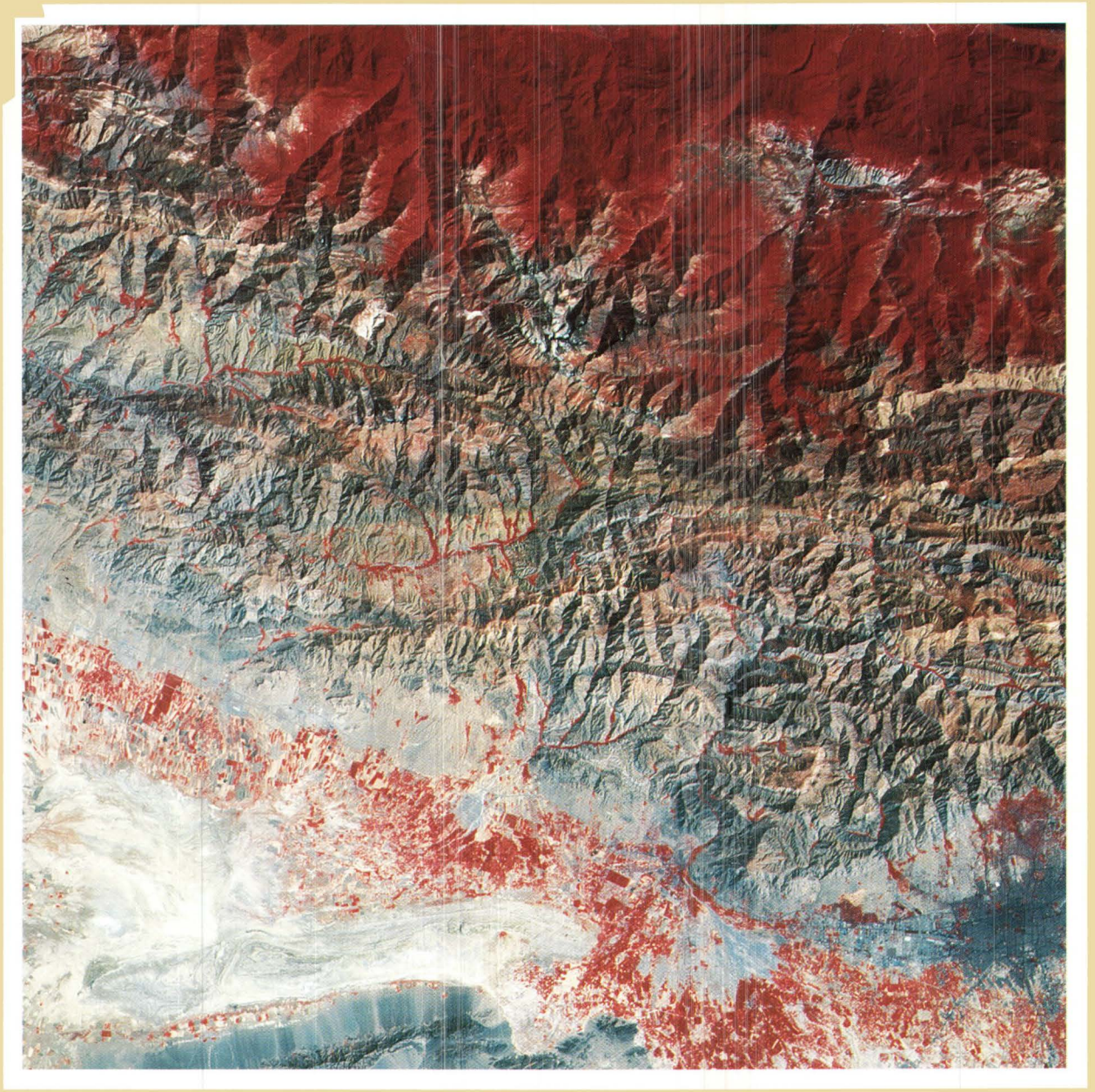

moisture. This abundant rainfall supports a heavy rainforest on the northern slopes of the Elburz Mountains, the rainforest appears as contiguous dark red areas in the upper-right portion of the images. The valley to the south of the mountains receives little or no precipitation because of the rain-shadow effect of the mountains. Agriculture in the valley depends on rainfall captured in the mountains and channeled to the valley floor and on nearby rivers and wells.

0 10 20 30

Scale 1 cm = 7.6 km

Landsat MSS
September 16, 1987

Central Saudi Arabia

0 10 20 30

Scale 1 cm = 6.9 km

Landsat MSS
December 25, 1972

The development of center-pivot irrigation agriculture in Saudi Arabia is shown in these images acquired on December 25, 1972, and February 15, 1986. The 1986 image shows the dramatic impact of center-pivot irrigation systems. Areas under this type of irrigation appear as red circles. Water from Saudi Arabia's aquifers is being used to grow crops such as wheat. The new irrigation systems extend beyond the image

areas throughout the Buraydah-Riyadh region of Saudi Arabia. This irrigation development resulted from the investment of part of Saudi Arabia's oil revenues in an effort to modernize agricultural practices. The cities of Buraydah and Unayzah can be seen at the western edge of each image and a new highway can be seen running across the lower part of the 1986 image to Unayzah.

0 10 20 30

Scale 1 cm = 6.9 km

Landsat MSS
February 15, 1986

Rondonia, Brazil

These images show a portion of the state of Rondonia, Brazil, in which deforestation of the tropical forests has taken place. Approximately 30 percent or 3,562,800 km^2 of the world's tropical forests are in Brazil. The estimated average deforestation rate from 1978 to 1988 was 15,000 km^2 per year. Systematic cutting of the forest vegetation starts along roads and then fans out to create the "feather" or "fishbone" pattern shown in the August 1, 1986, and June 22, 1992 images. The deforested land and urban areas appear as light blue; healthy vegetation appears red. Both MSS and TM data are used to demonstrate how this activity can be monitored.

Scale 1 cm = 9 km

Landsat MSS
June 19, 1975

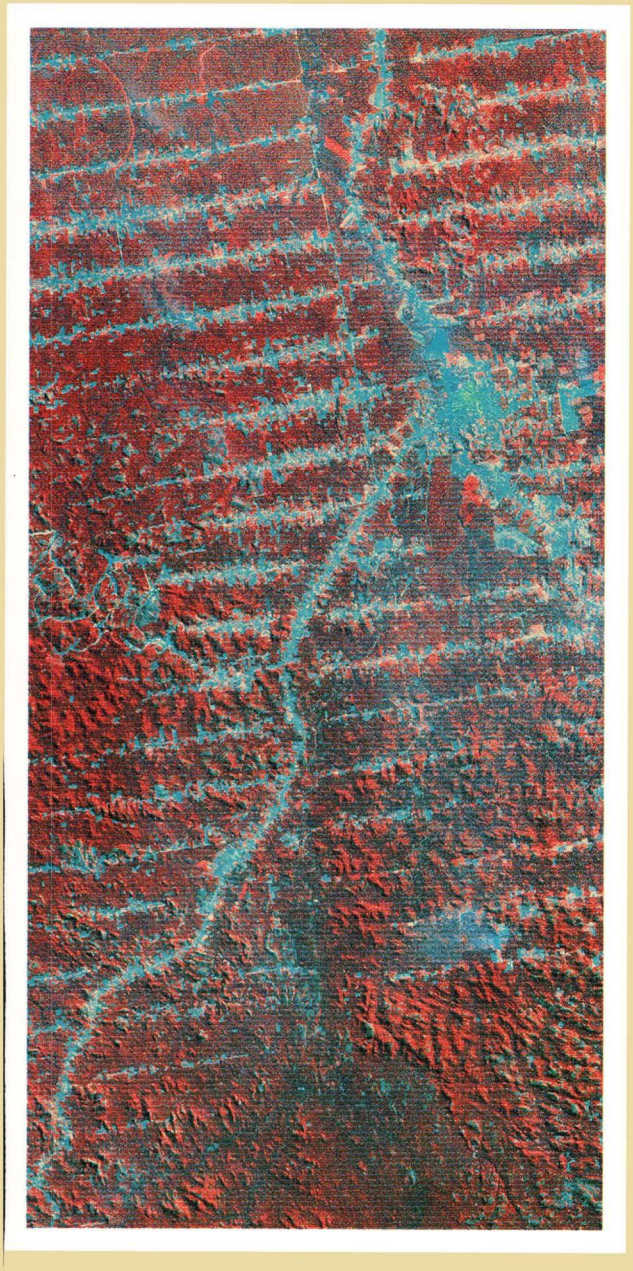

Landsat MSS
August 1, 1986

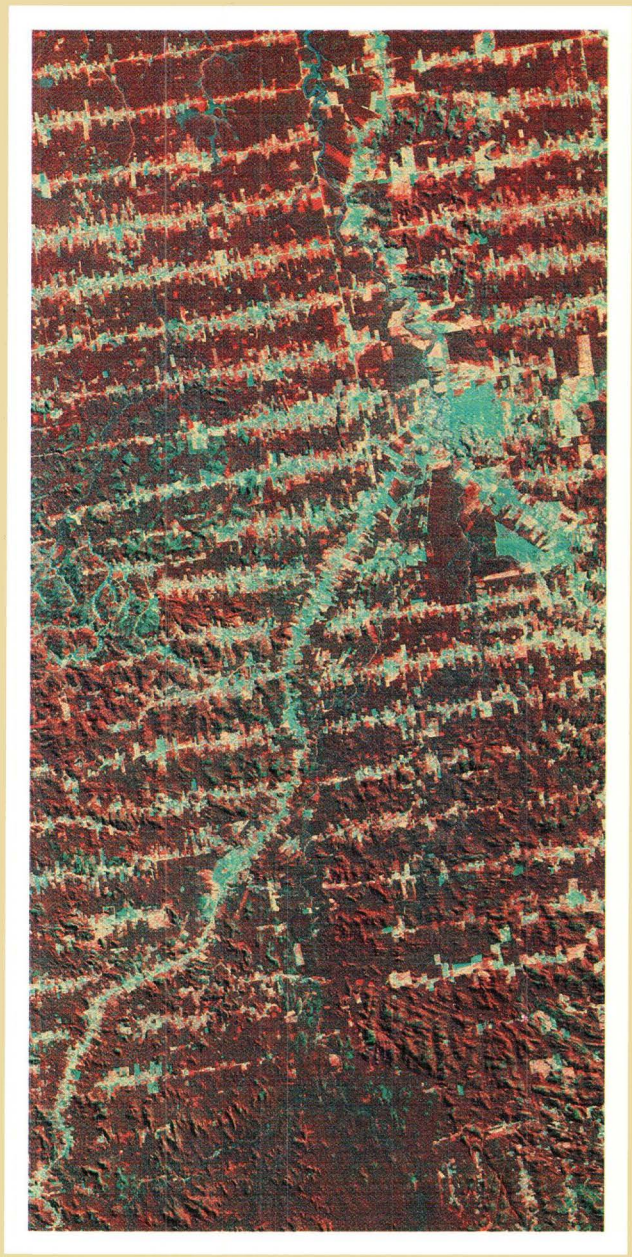

Landsat TM
June 22, 1992

Forest Change
Natural Disasters

Mount St. Helens, Washington, USA

Three images document the changes in the vicinity of Mount St. Helens during the last 15 years. The September 15, 1973, image shows Mount St. Helens and adjacent forest land before the eruption on May 18, 1980. The May 22, 1983, image shows the extent of volcanic debris caused by the explosive eruption, with the collapsed north edge of the crater clearly evident. The area north of the crater is the most devastated, with mudslides, volcanic ash, and mud-laden rivers shown as grayish-blue areas. Spirit, Coldwater, and South Fork Castle Creek Lakes north of the volcano can be seen in the 1973 image, but are partially obscured in the May 22, 1983, image by the debris and ash flows. Swift Reservoir and Yale Lake, south of the mountain, received silt- and ash-laden runoff from the damaged areas. The volcano ejected an estimated 400 million tons of ash into the atmosphere and devastated an area of 600 km^2.

The August 31, 1988, image shows some vegetation regrowth, light red and pink, in the devastated area. The patchwork block patterns in the forested land east of Mount St. Helens are areas where timber has been removed. This image shows an increase in the timber harvested from land in this region when compared with the September 15, 1973, image. The city of Portland, Oregon, is visible in the bottom of each image as are the Columbia and Willamette Rivers.

Scale 1 cm = 9.5 km.

Landsat MSS
September 15, 1973

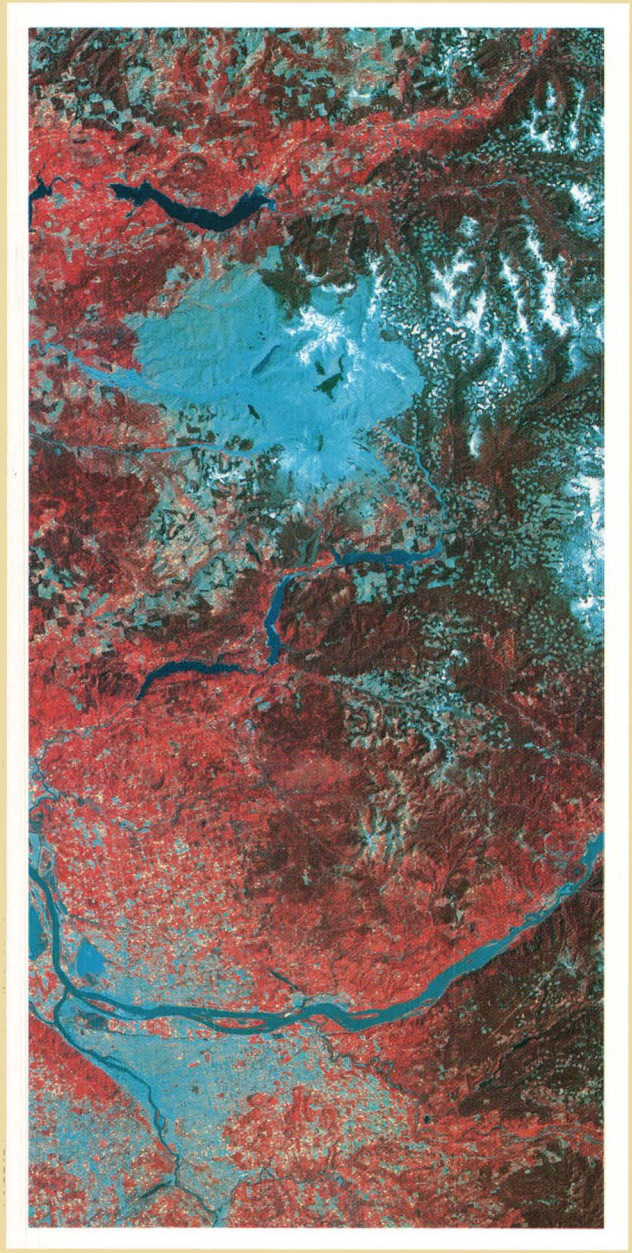

Landsat MSS
May 22, 1983

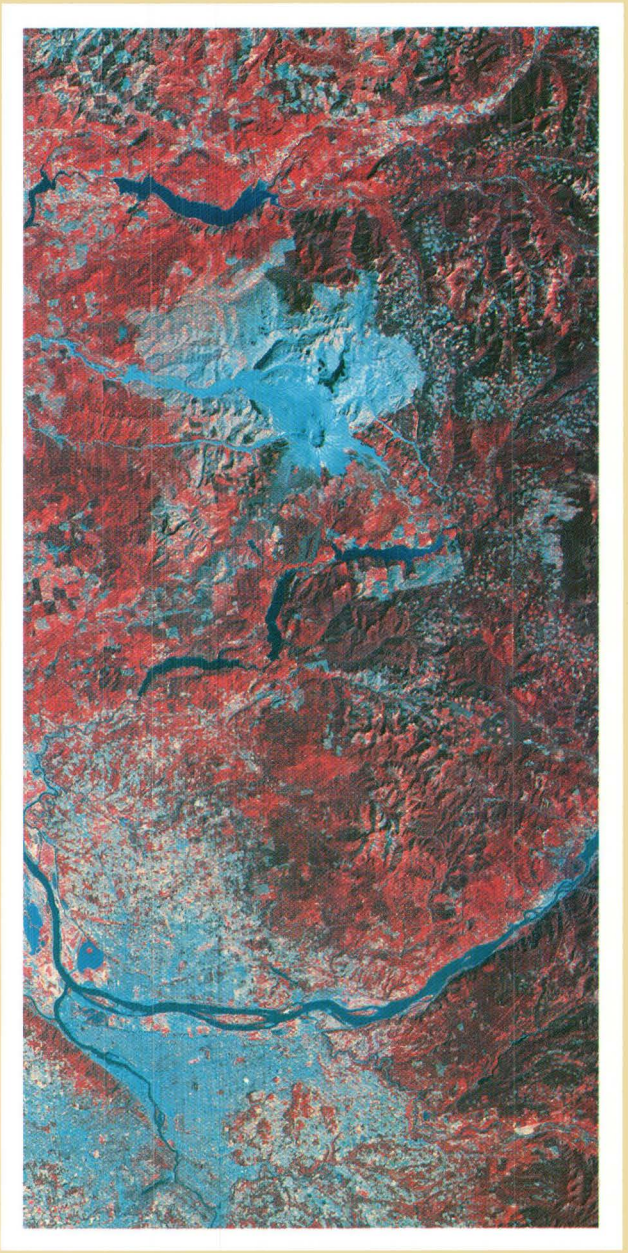

Landsat MSS
August 31, 1988

Yellowstone National Park, Wyoming, USA

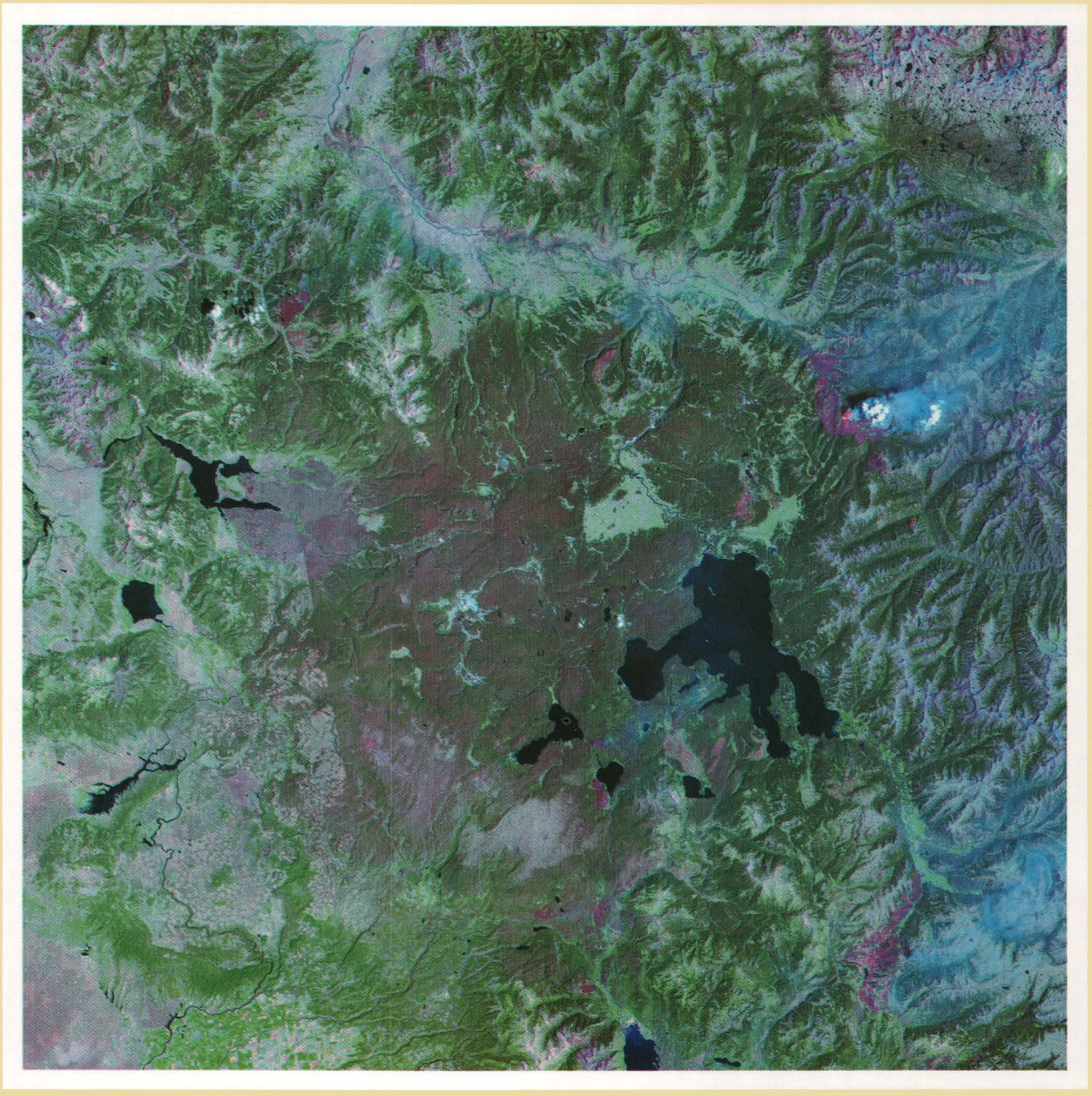

0 10 20 30 40

Scale 1 cm = 9.5 km

Landsat TM
July 22, 1988

These images from July 22, 1988, and October 2, 1988, document the dramatic forest fires that occurred in and adjacent to Yellowstone National Park. These images were created using bands 7, 4, and 3 to make the burned areas easier to identify. This band combination depicts water bodies as dark blue, healthy vegetation in shades of green (conifer forest in dark green and grassland in light green tones), and burned vegetation in shades of red. Yellowstone Lake appears as the large dark blue feature in the center portion of the image. The lake on the left edge of the image is Hebgen Lake.

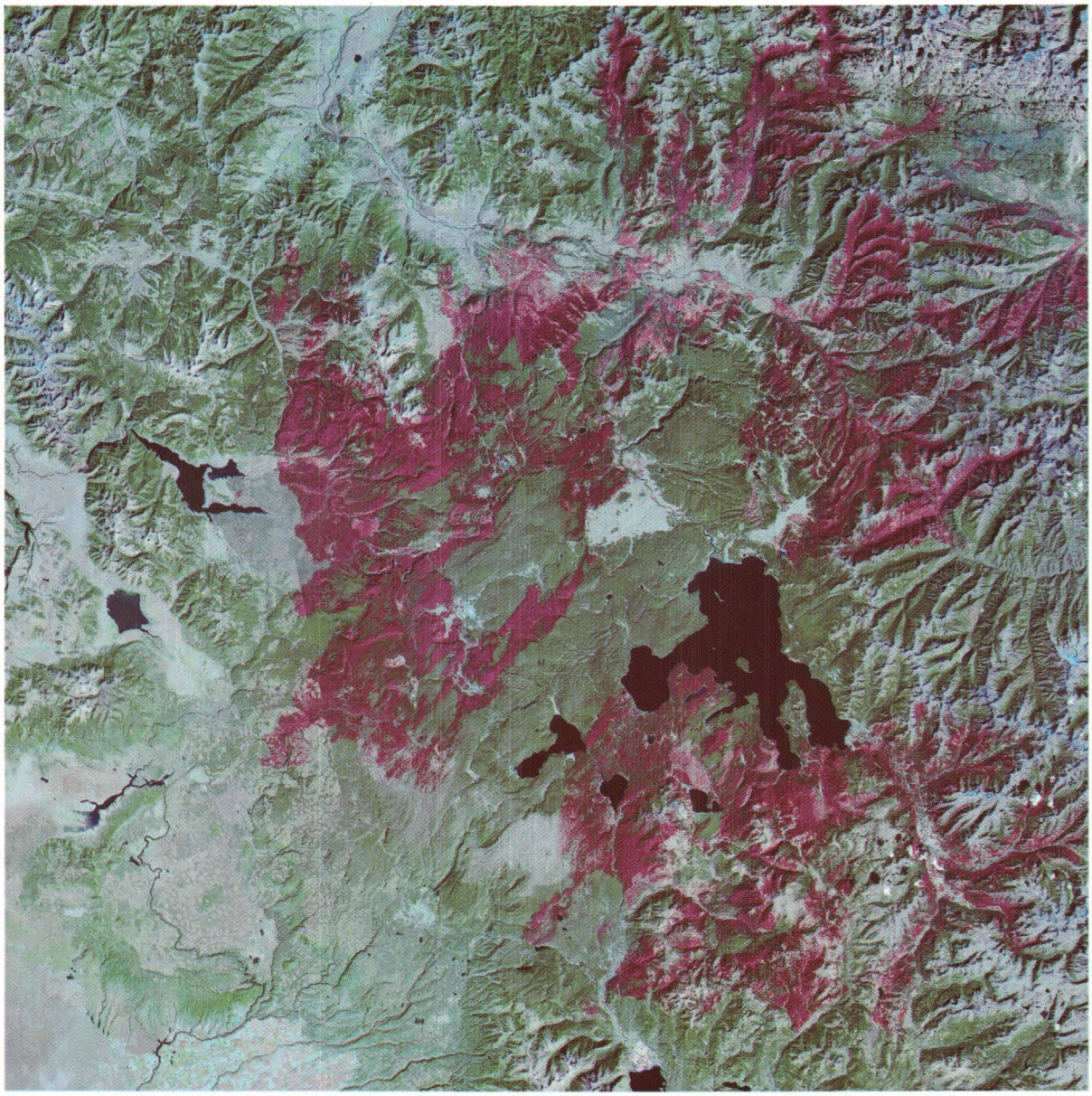

0 10 20 30 40

Scale 1 cm = 9.5 km

The first fires of the fire season are documented on the July image. The Clover-Mist fire clearly appears in the right-center portion of the image. Smoke can be seen rising from the burned area.

The extent of the fires can be assessed from the October image. In this image all the fires have been extinguished and the burned areas are easily identified by the purple tones. Eight major fires swept through nearly half of the park's 2.2 million acres.

Landsat TM
October 2, 1988

Kuwait

These images illustrate the extent of the oil fires in Kuwait ignited during the Persian Gulf war. The August 31, 1990, image shows the capital city of Kuwait in the upper-center part of the image. In the February 23, 1991, image the Kuwaiti coastline below the city of Kuwait is obscured by smoke plumes from burning oil wells. The November 14, 1991, image was acquired after the fires had been extinguished. The results of the oil fires are evident by the black oil and soot deposits on the land surface, particularly below the city of Kuwait.

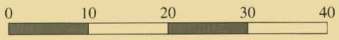

Scale 1 cm = 9.5 km

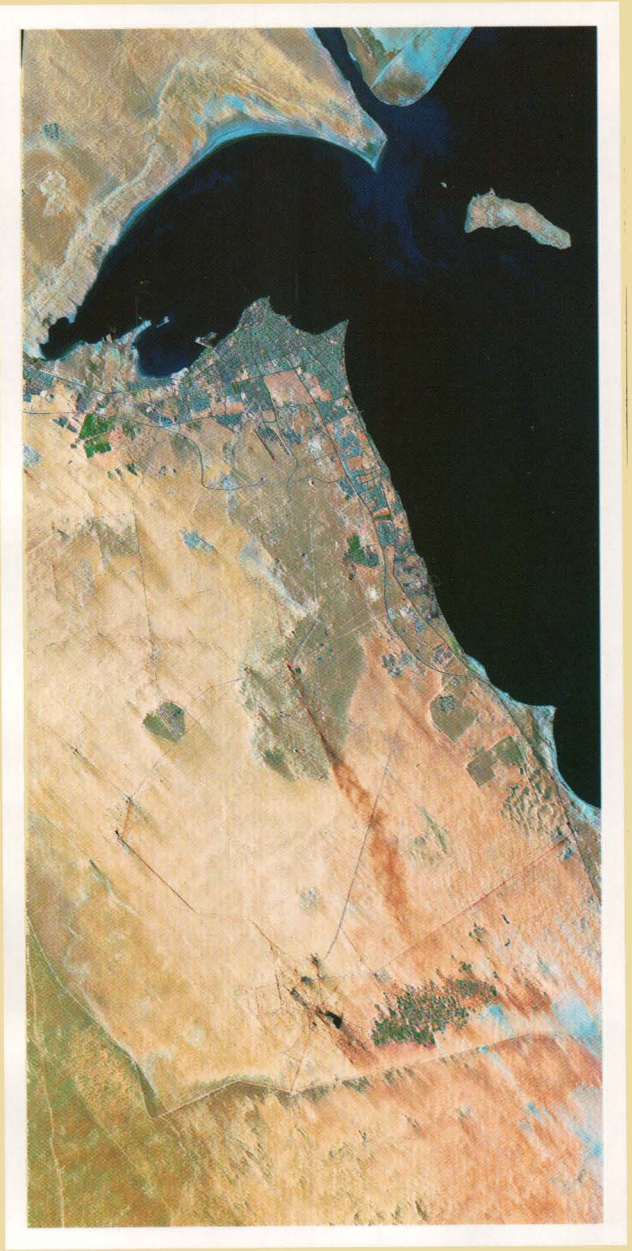

Landsat TM
August 31, 1990

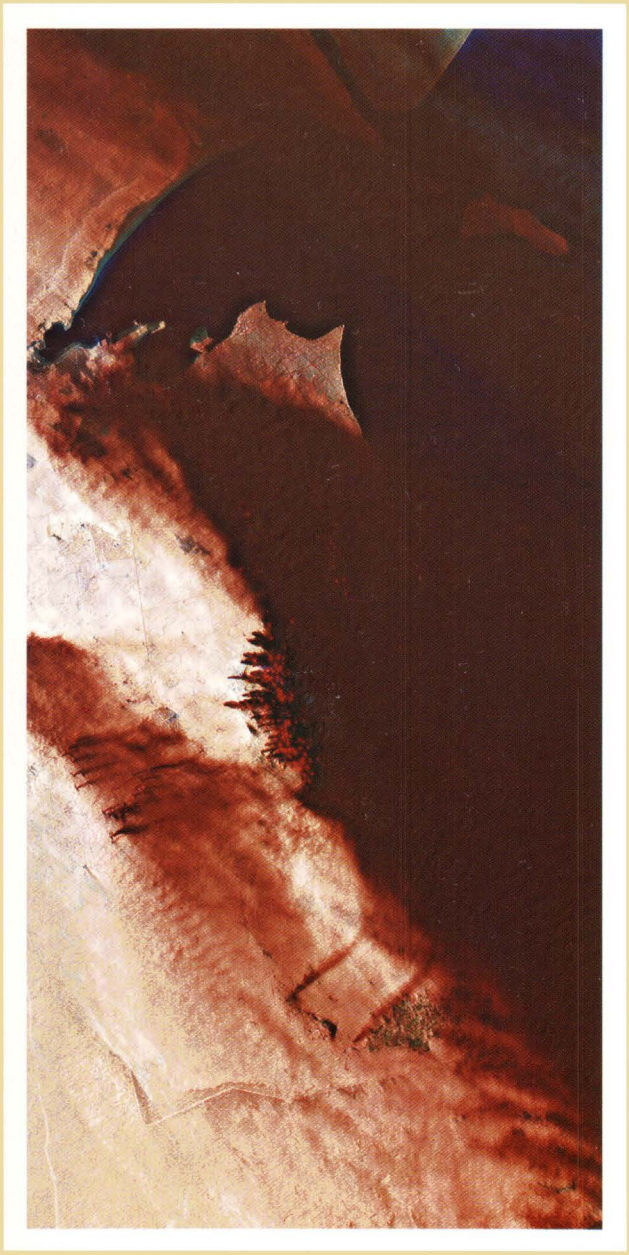

Landsat TM
February 23, 1991

Landsat TM
November 14, 1991

Dallas-Fort Worth, Texas, USA

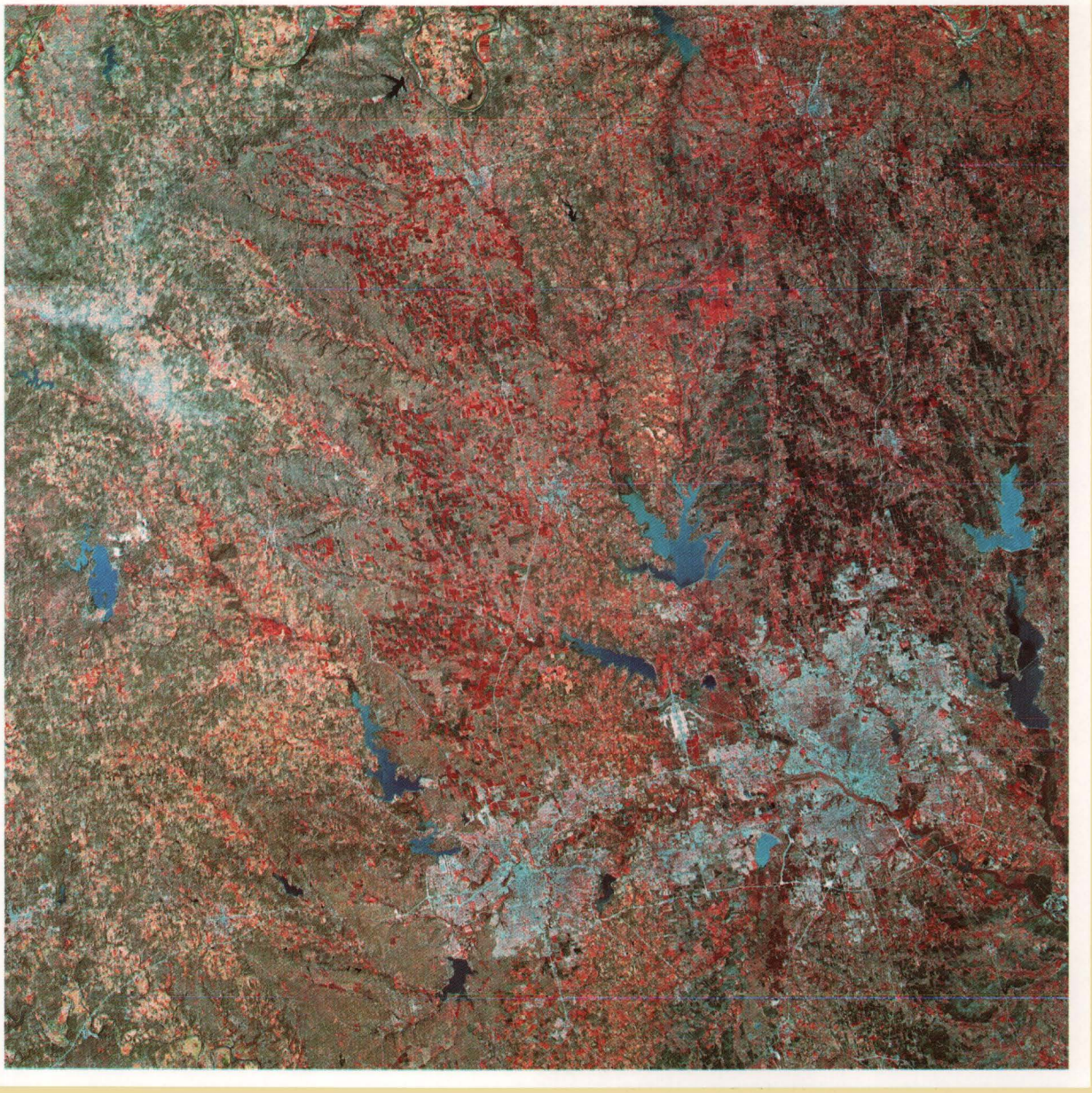

0 10 20 30 40

Scale 1 cm = 9.5 km

Landsat MSS
March 12, 1974

Dallas-Fort Worth, Texas, has grown significantly in the last 20 years. These images acquired on March 12, 1974, and on March 22, 1989, show the expansion of urban areas into the surrounding countryside. The population of this metropolitan area grew from 2,378,000 in 1970 to 3,776,000 by 1988. The

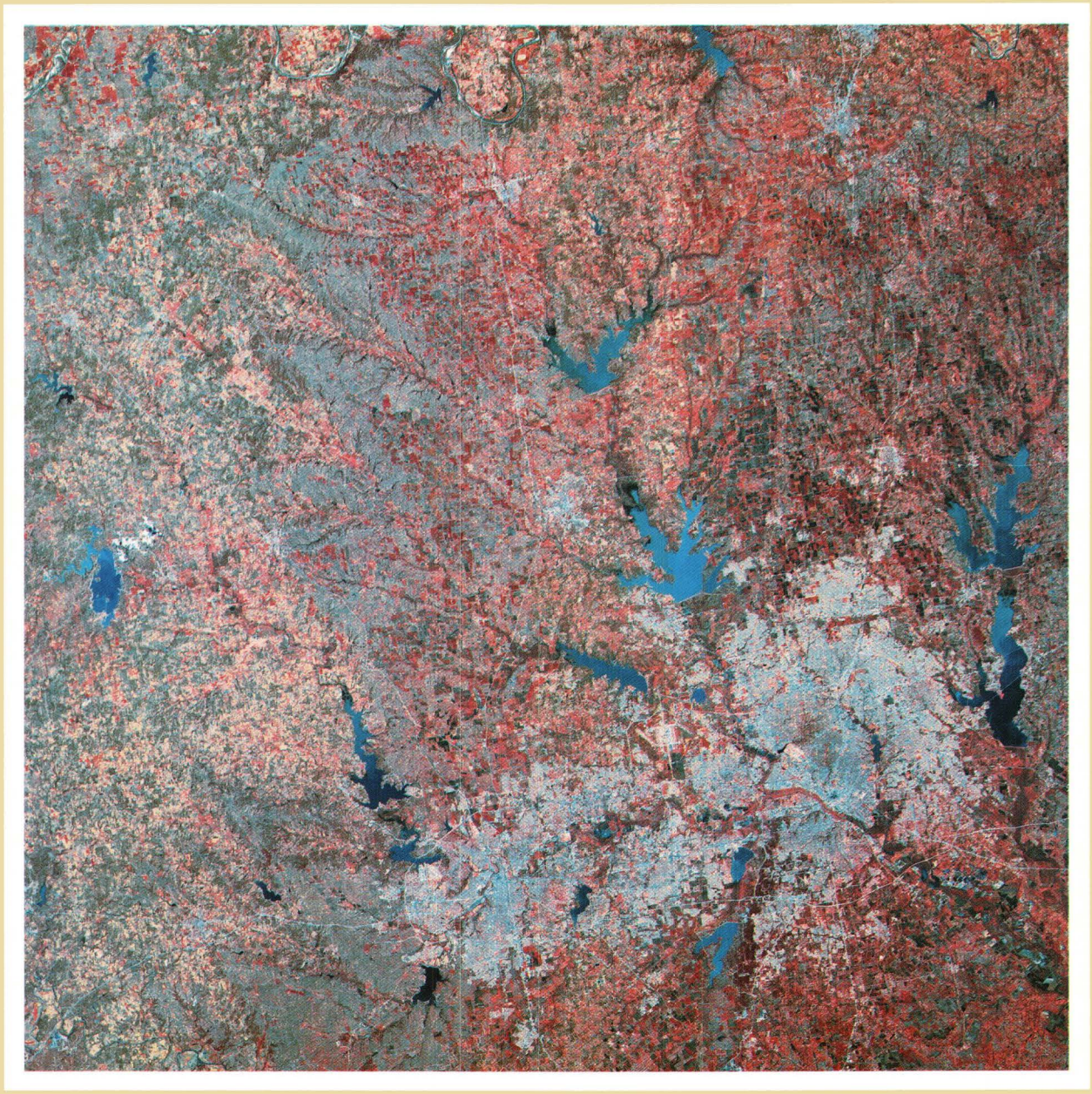

Ray Roberts Reservoir, northwest of Dallas, and Joe Pool Lake, southwest of Dallas, have been constructed since 1974. Also, the recently constructed Dallas-Fort Worth International Airport can be seen north of the Dallas-Fort Worth metropolitan area.

Scale 1 cm = 9.5 km

Landsat MSS
March 22, 1989

South-Central Texas, USA

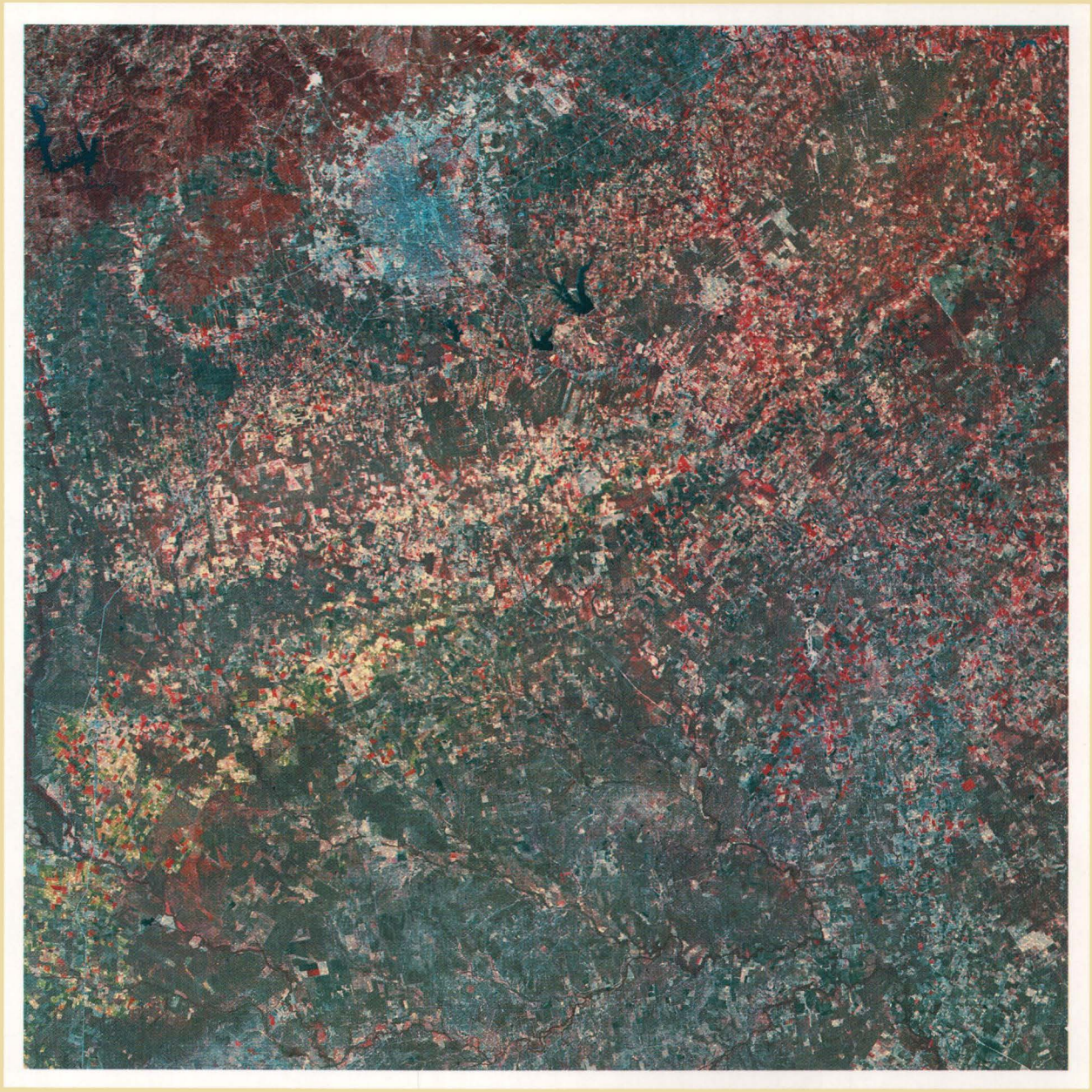

0 10 20 30 40

Scale 1 cm = 9.5 km

Images acquired over south-central Texas show the development of a new reservoir on the Frio River between February 4, 1974, and March 19, 1988. The resulting reservoir is Choke Canyon Reservoir near the town of Beeville, Texas.

Landsat MSS
February 4, 1974

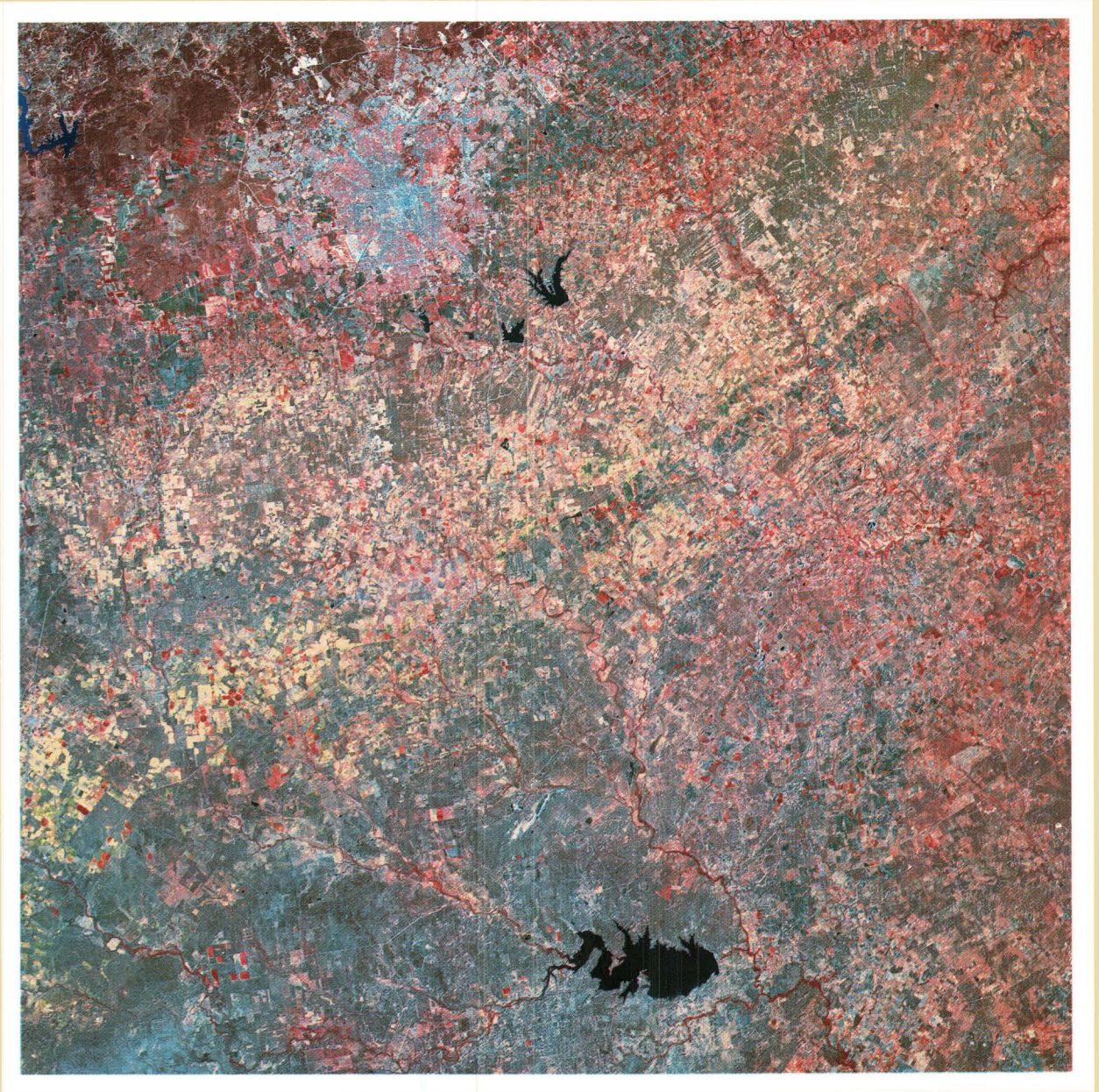

San Antonio, Texas, is shown in the upper-left-hand corner of each image. Note the dramatic growth of the city from approximately 654,000 in 1970 to more than 936,000 in 1990.

0 10 20 30 40

Scale 1 cm = 9.5 km

Landsat MSS
March 19, 1988

Lake Chad, West Africa

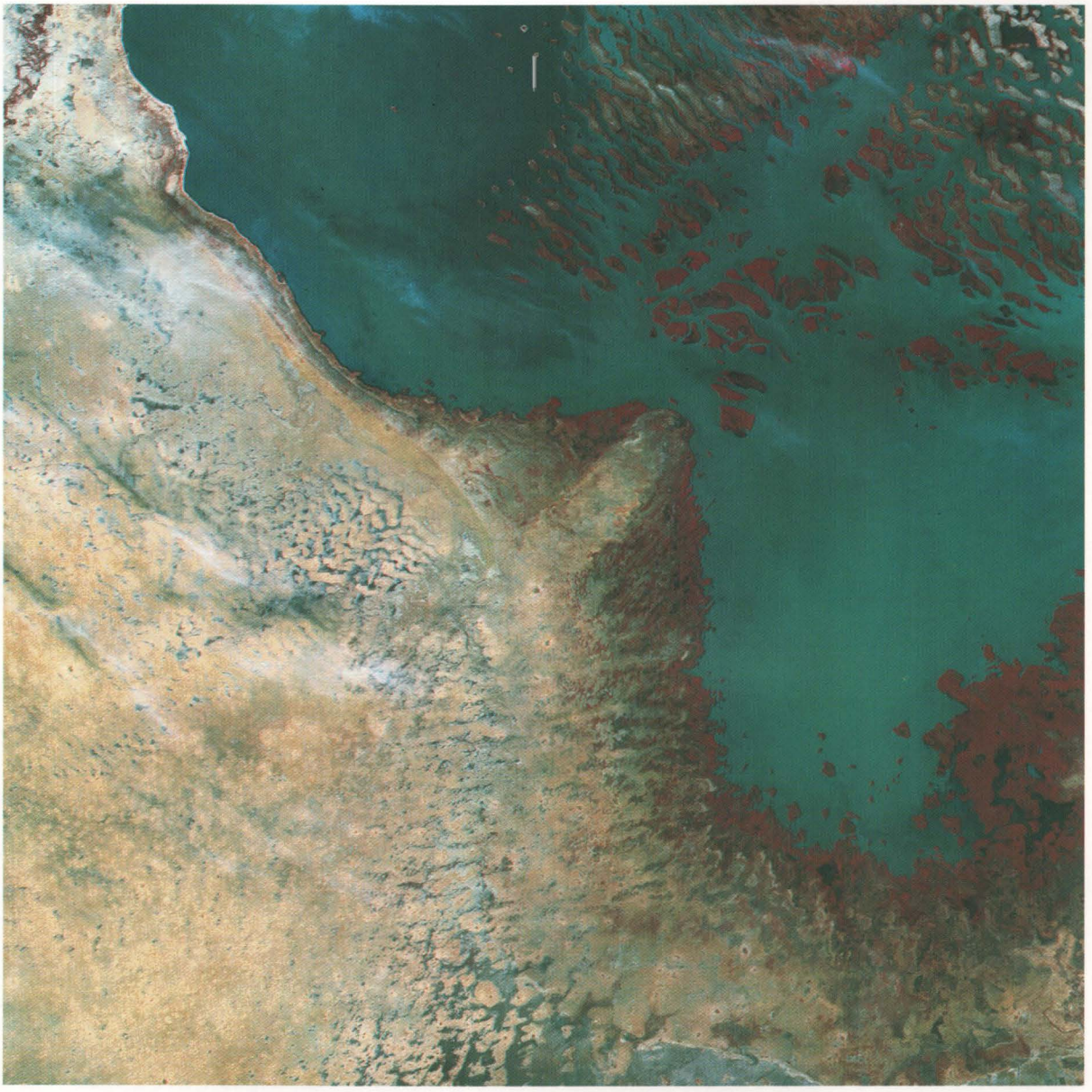

0 10 20 30

Scale 1 cm = 8 km

Landsat MSS
December 8, 1972

Lake Chad, which forms part of the borders of Cameroon, Chad, Niger, and Nigeria, has decreased considerably since the 1960's because of a prolonged drought. Historically, the area of the lake can fluctuate thousands of square kilometers between the dry season and the end of the rainy season. Reasons for these fluctuations are the relative shallowness of the lake, the diversion of water for irrigation, and climate. The lake covered approximately 26,000 square kilometers in the early 1960's. The December 8, 1972 image, shows the lake level lower than the mid-1960's level. After the extended drought of the 1970's and mid-1980's, the size of the lake

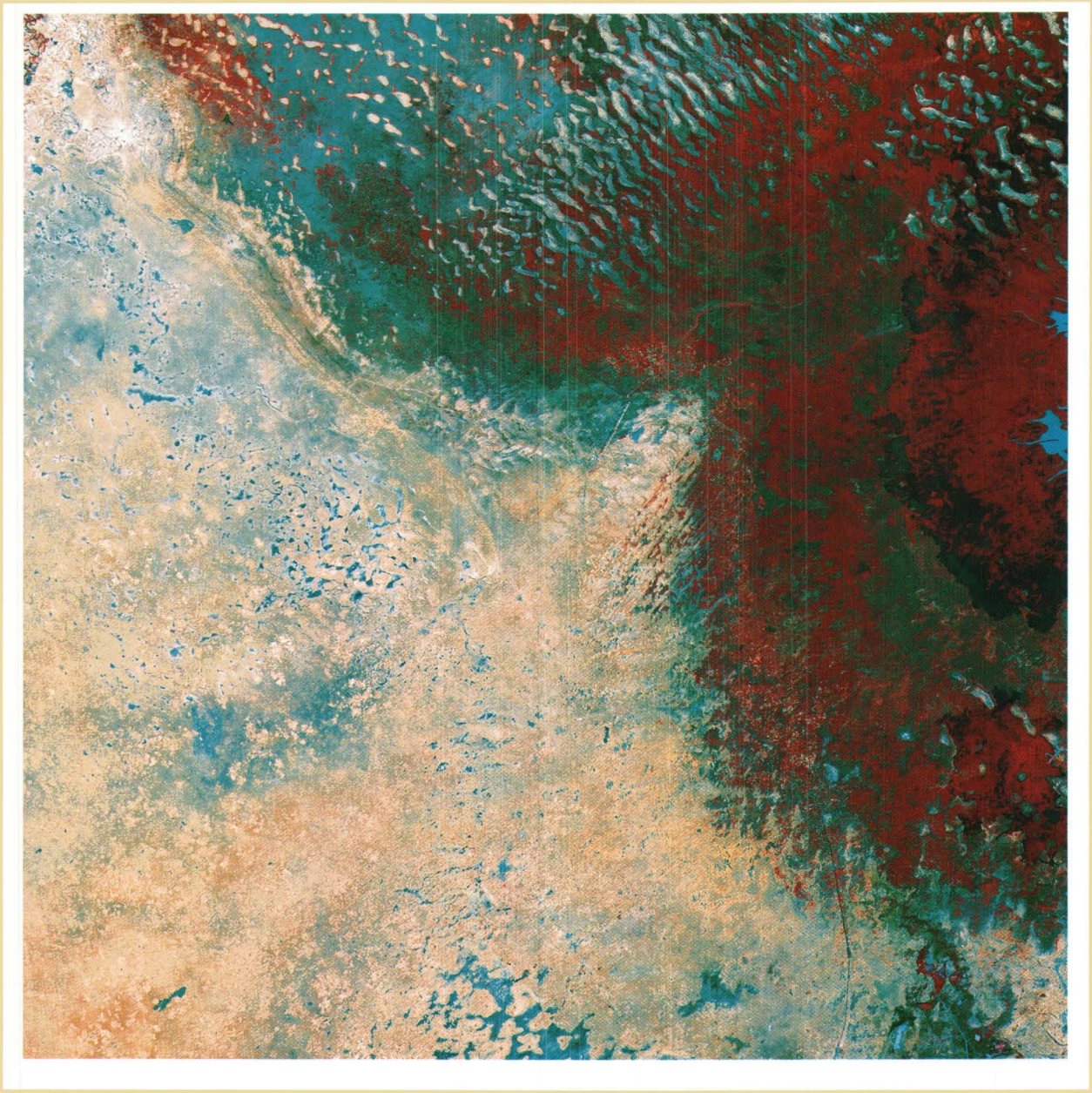

shrunk to less than 3000 square kilometers, the light blue area at right-center in the October 1987 image.

The Chari and Logone rivers, which contribute more than 80 percent of the total water supply for Lake Chad, were reduced to a trickle during the drought years. Many ancient dunes, long covered by the waters of the lake, are visible in the 1987 image. Note the old beach marks along the western side of the lake basin in 1987. Much of the former lake has been replaced by wetlands, indicating that the water table remains near the surface.

0 10 20 30

Scale 1 cm = 8 km

Landsat MSS
October 14, 1987

Aral Sea, Kazakhstan

0 10 20 30 40

Scale 1 cm = 9.5 km

Landsat MSS
May 29, 1973

The change in the shoreline of the Aral Sea is shown in May 29, 1973, and August 19, 1987, images. Over the past 30 years water has been diverted from the Amudar'ya and the Syr-Dar'ya rivers feeding the Aral to irrigate millions of acres of land for cotton and rice production in Central Asia. The diversion of water has caused a loss of over 60 percent of the lake's water since the 1960's. The lake has shrunk from over 65,000 square kilometers to less than half that size, exposing large areas of the lake bed. From 1973 to 1987 the Aral dropped from fourth to sixth among the world's largest lakes.

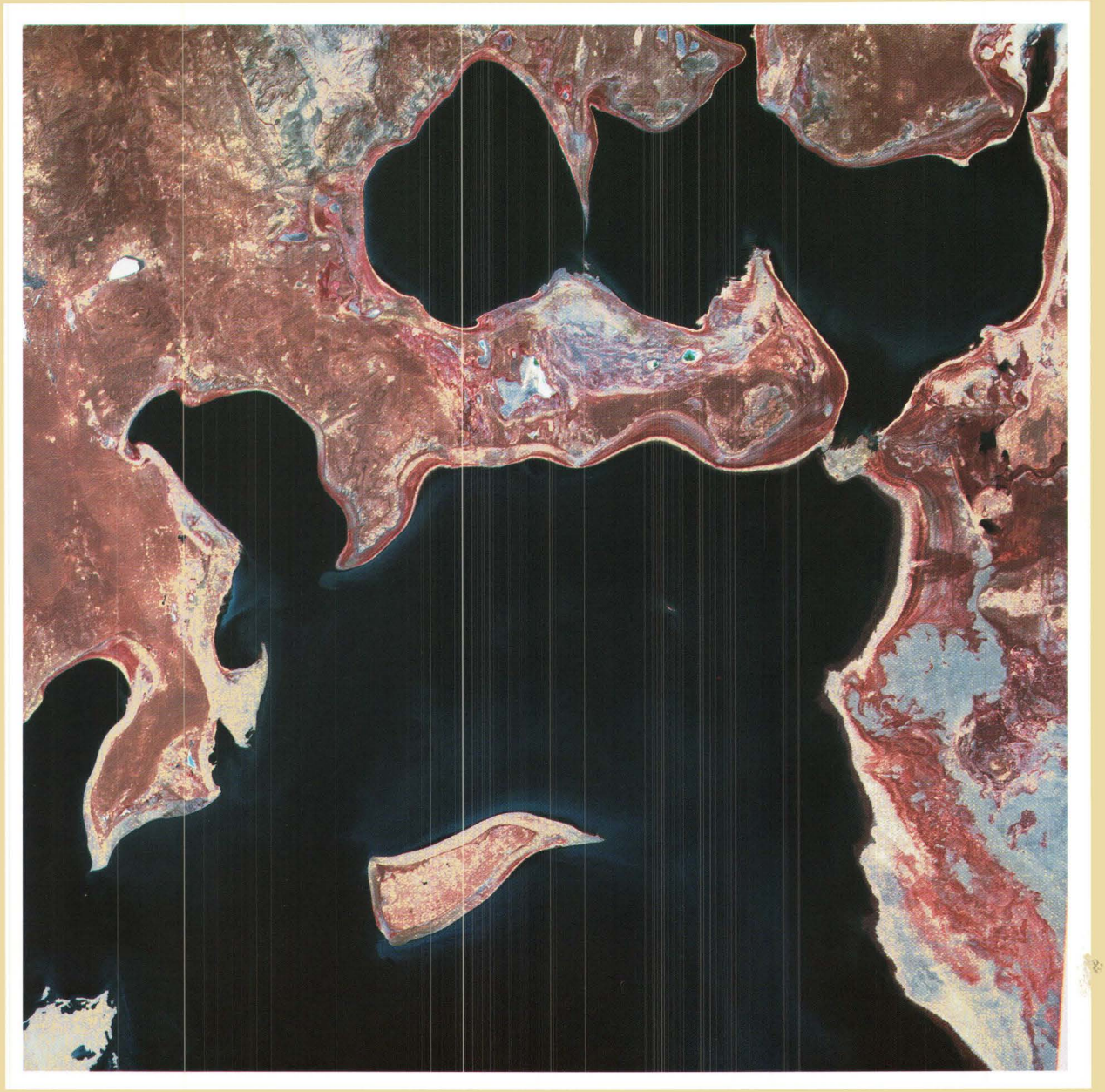

The environmental consequences of the shrinkage include doubling of the salt concentrations in the lake from 10 percent to more than 23 percent, which has contributed to the devastation of a once thriving fishery and a shift in the local climate. Summers are reportedly hotter and drier and the winters are colder and longer. Dust storms of salt particles and pesticide residues, originating from the exposed lake bed, create air pollution for hundreds of kilometers, resulting in widespread nutritional and respiratory ailments.

Scale 1 cm = 9.5 km

Landsat MSS
August 19, 1987

Kara-Bogaz-Gol, Caspian Sea,Turkmenistan

0 10 20 30

Scale 1 cm = 7.6 km

Landsat MSS
December 4, 1972

The depletion of water in the Kara-Bogaz-Gol (KBG), an inlet bay on the eastern side of the Caspian Sea, is shown. The KBG has been used as an evaporating basin for salts since the early 1920's. In March 1980 a dike was completed across the strait that connected the KBG with the Caspian Sea in an attempt to

help stabilize the water level of the Caspian Sea. The original estimate of 25 years for the water in the KBG to evaporate was optimistic. The impact was more dramatic, resulting in the complete evaporation of the water in the KBG by late 1983.

0 10 20 30

Scale 1 cm = 7.6 km

Landsat MSS
September 25, 1987

Lake Turkana, Kenya

0 10 20

Scale 1 cm = 4.6 km

Landsat MSS
February 1, 1973

Lake Turkana, formerly Lake Rudolf, lies in the Rift Valley of East Africa. It is approximately 240 km long and 40 km wide with an average depth of about 35 meters. Images from February 1, 1973, and January 12, 1989, show changes on the delta of the Omo River on the north shores of Lake Turkana. The Omo River provides more than 80 percent of the fresh water to the lake, which has no outlet and lies in a very arid area of Africa.

The river delta increased by approximately 380 square kilometers between 1973 and 1989. This increase is largely

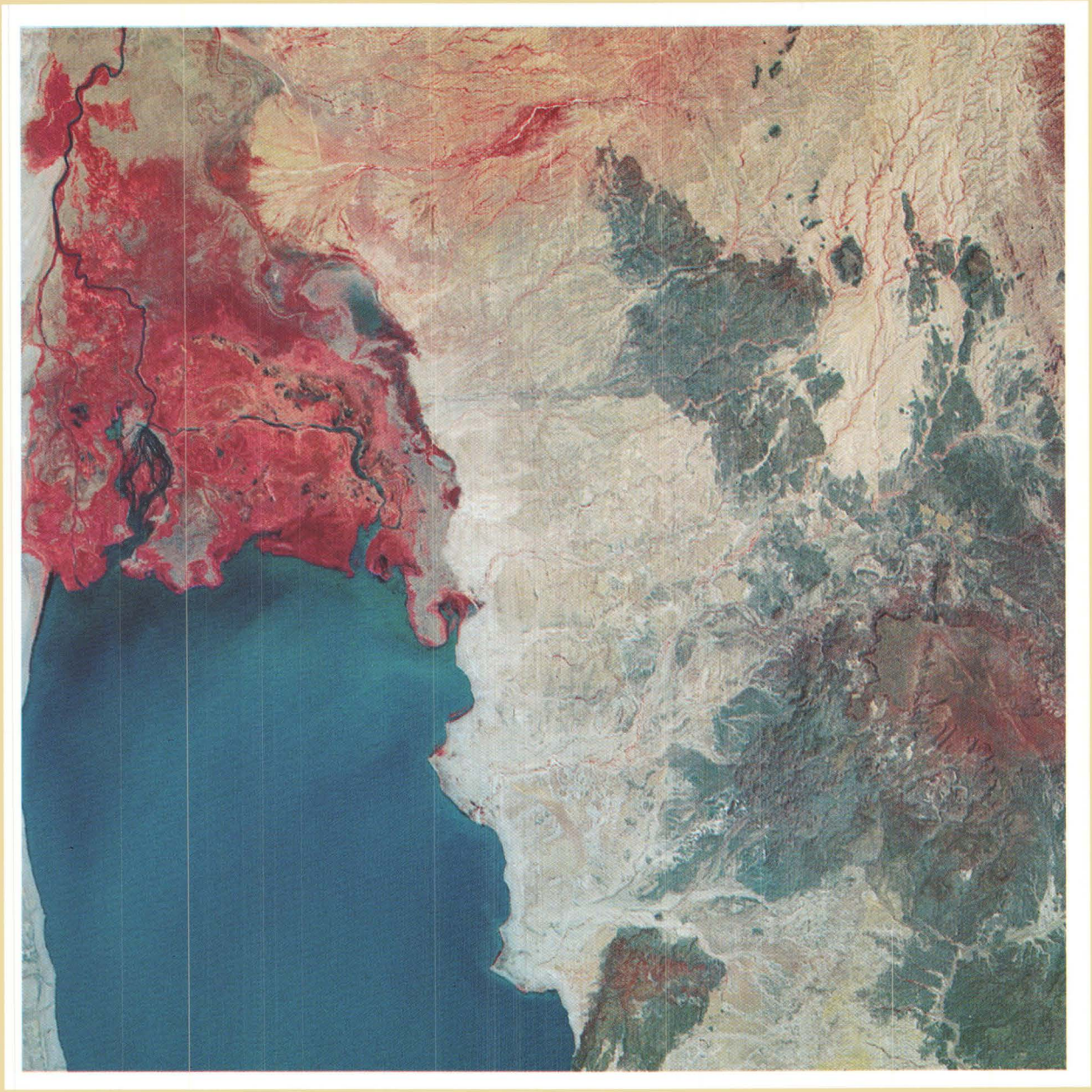

due to a precipitous drop in the water level, exposing the submerged portions of the delta. Aquatic vegetation has taken hold on the emerging delta. Prolonged drought, and the damming of three rivers for irrigation near the southern reaches of the lake have contributed to the lake's decline. Increasing water salinity threatens the lake's wildlife. The El Molo, Africa's smallest tribe with just over 200 members, live along the lake's southeastern shore. They fish and hunt Nile crocodiles along the lake shore.

0 10 20

Scale 1 cm = 4.6 km

Landsat MSS
January 12, 1989

Great Salt Lake, Utah, USA

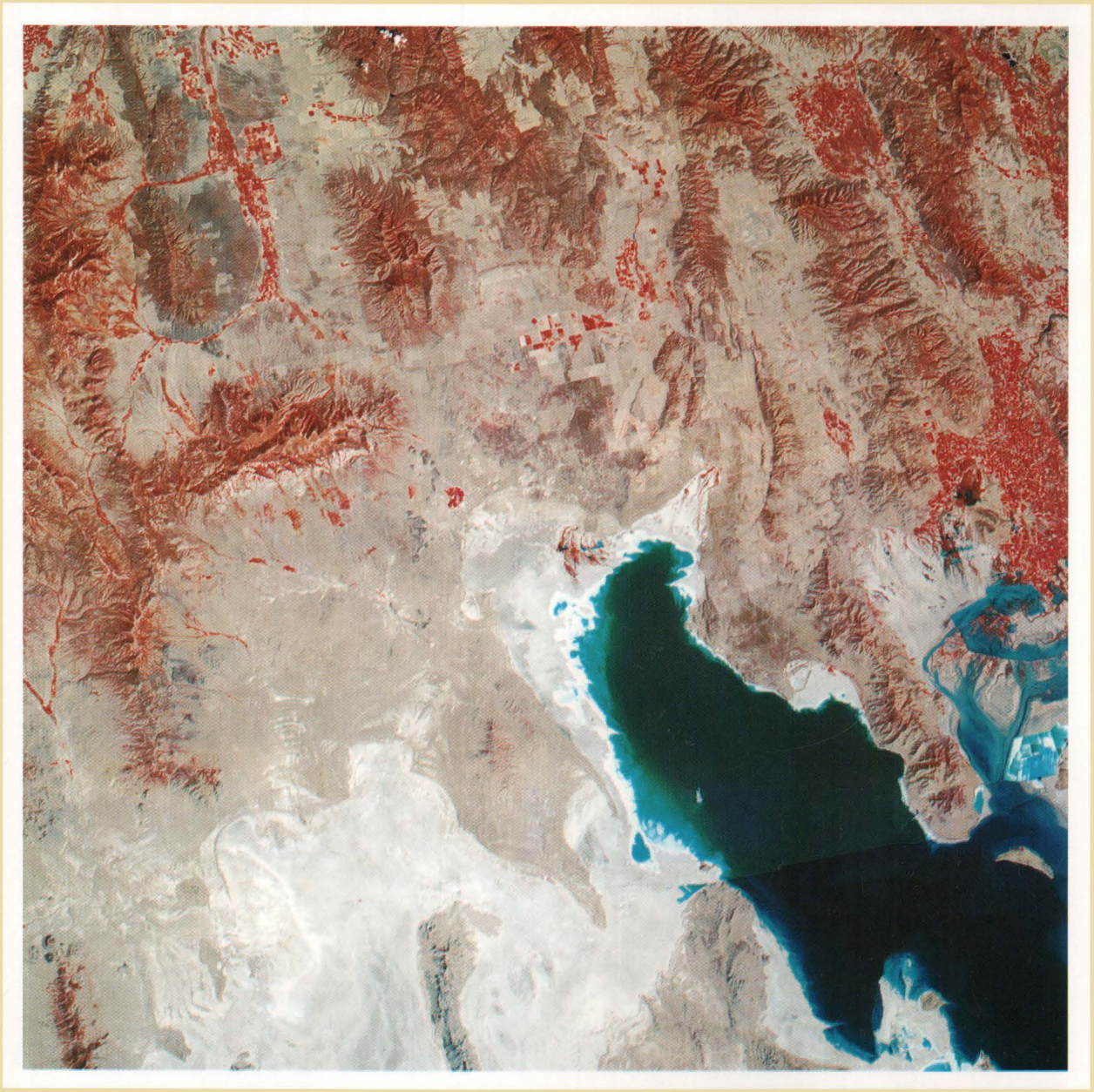

0 10 20 30 40

Scale 1 cm = 9.5 km

Landsat MSS
September 13, 1972

These images from 1972 and 1988 show the dramatic increase of the surface area of the Great Salt Lake in Utah. The rise in water level has increased the size of the lake to more than 5,900 square kilometers, from a low in 1963 of 2,300 square kilometers, and caused millions of dollars in damage by flooding highways, homes, wildlife refuges, and railways near the lake. In May 1986, the Utah legislature approved a project

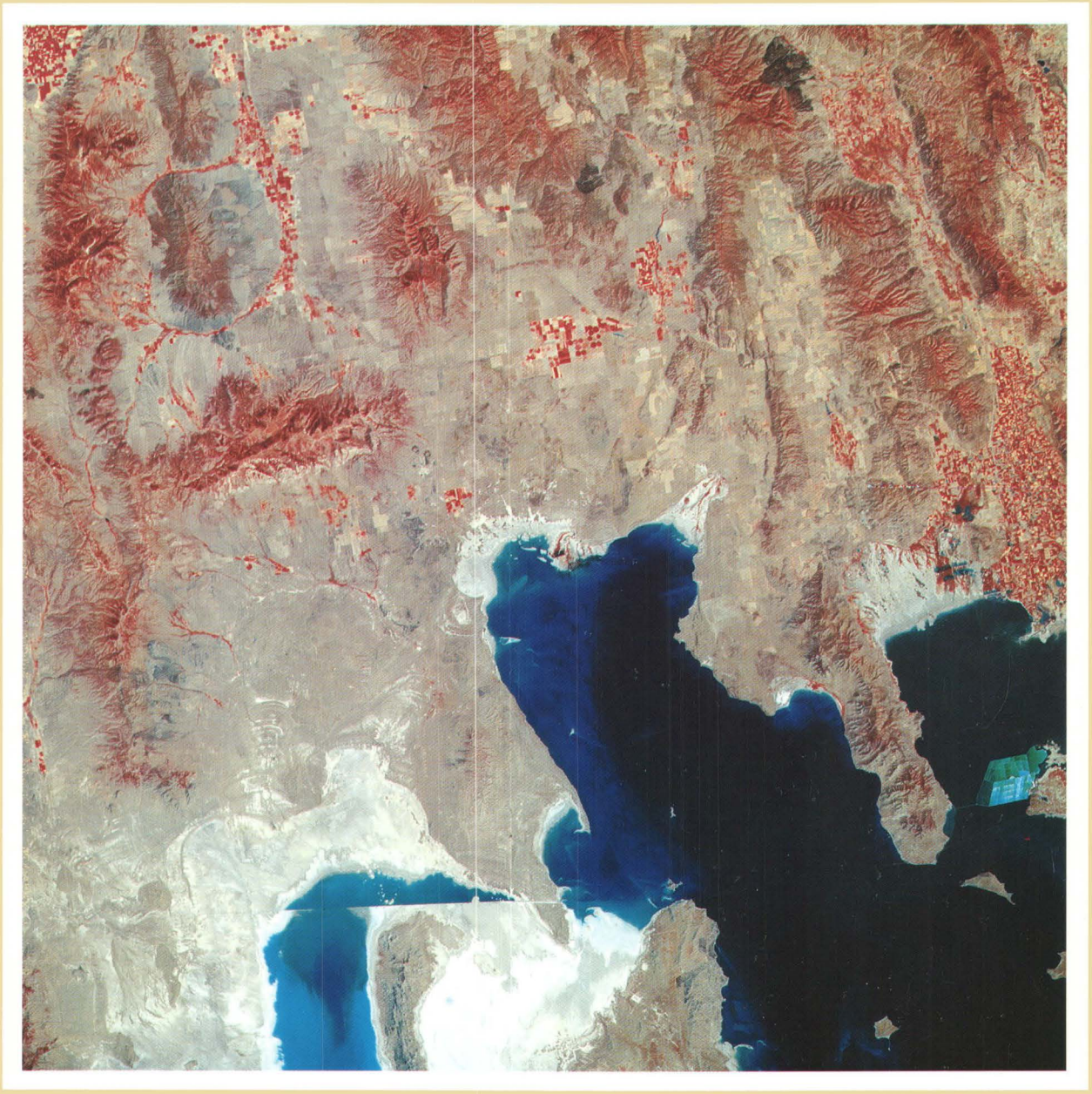

to pump excess water out of the Great Salt Lake onto a portion of the Bonneville salt flats west of the lake. This new water body, Newfoundland Evaporation Basin, which can be seen to the west of the Great Salt Lake in the 1988 image, was constructed to help control the level of the lake.

0 10 20 30 40

Scale 1 cm = 9.5 km

Landsat MSS
August 14, 1988

Hubbard Glacier, Alaska, USA

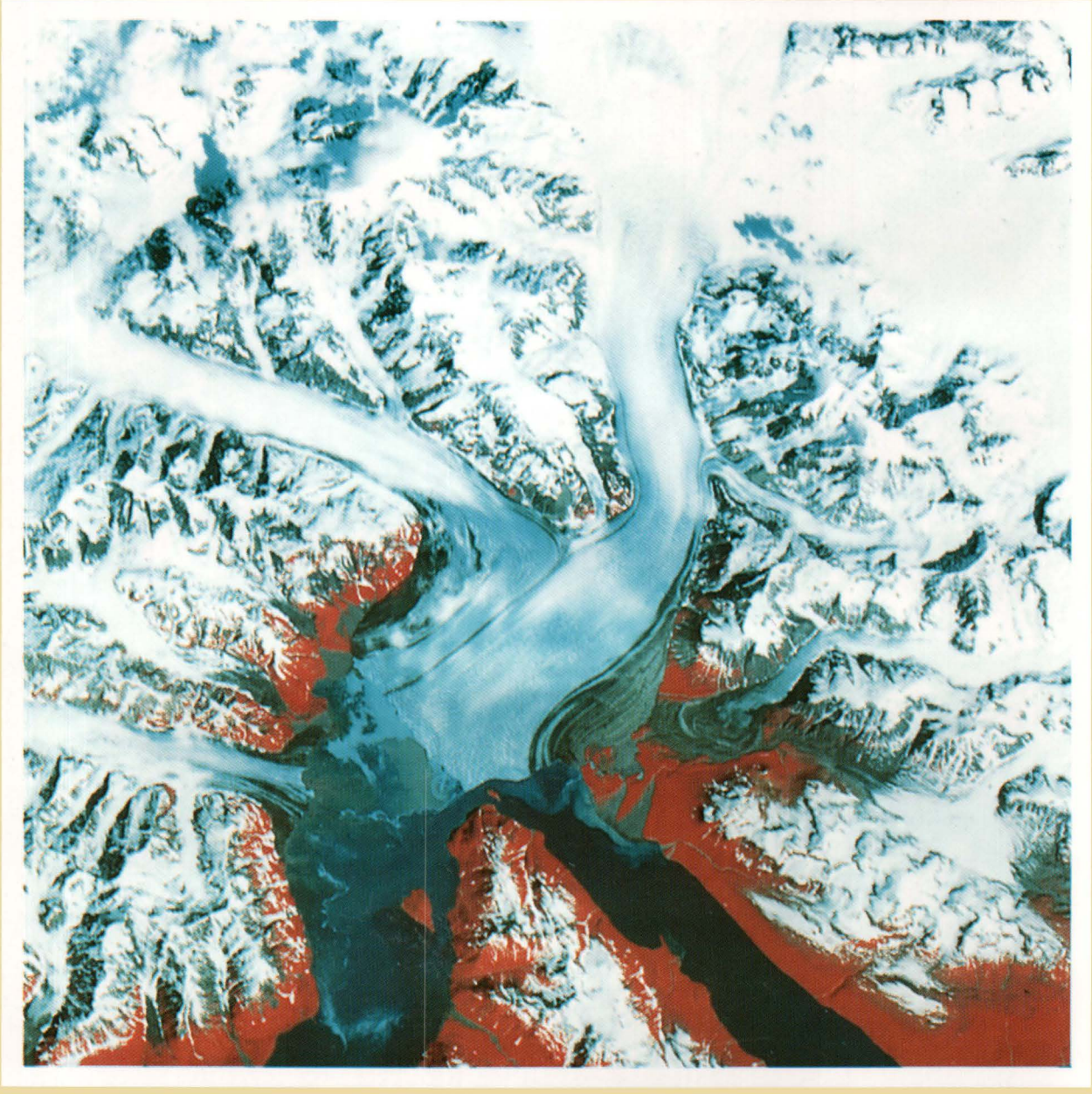

0 5 10

Scale 1 cm = 2.5 km

Landsat TM
August 7, 1985

In 1986 the Hubbard Glacier in the Wrangell-St. Elias National Park near Yakutat, Alaska, surged forward, blocking Russell Fiord. Russell Fiord, a saltwater fiord, began to rise from the runoff of the surrounding area and became known as "Russell Lake." The runoff reduced the salinity of the lake, endangering such sea life as seals and porpoises. Another concern over the

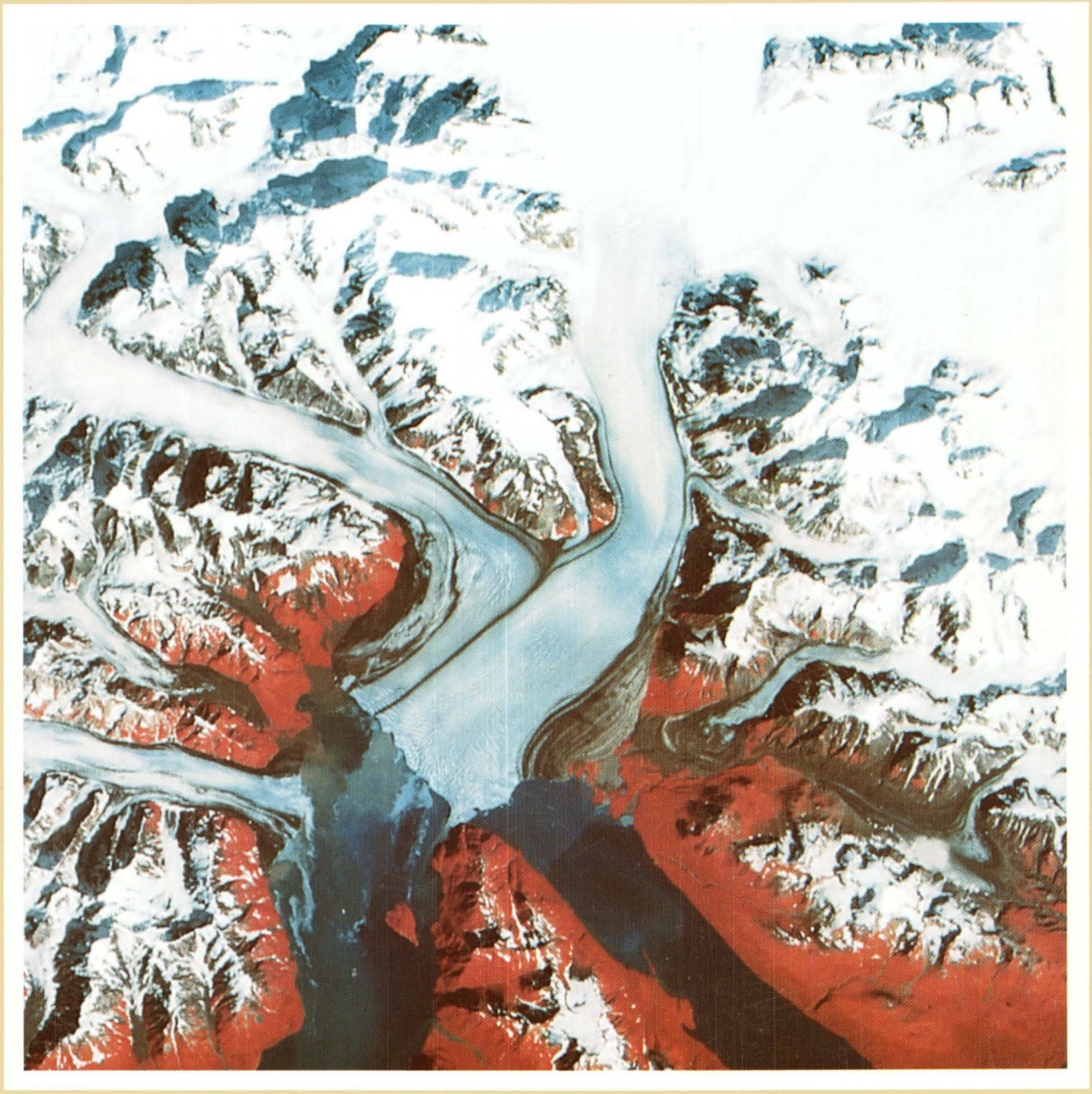

rising water level was the possibility of the fiord's draining southward into the Situk River and affecting the area's fishery. Before the ice dam broke on October 8, 1986, the water level of Russell Fiord rose more than 25 meters. These images show the area prior to the surge and while the fiord was blocked.

0 5 10

Scale 1 cm = 2.5 km

Landsat TM
September 11, 1986

Access to Landsat Data

Information on the availability of Landsat and other types of images can be obtained from the U.S. Geological Survey's EROS Data Center.

Mail: U.S. Geological Survey
EROS Data Center
Customer Services
Sioux Falls, SD 57198

Telephone: 605-594-6151
FAX: 605-594-6589
E-mail: custserv@edcserver1.cr.usgs.gov

Information on the availability of Landsat images can also be acquired through the Global Land Information System (GLIS). GLIS is an interactive computer system that provides information on land data sets to a wide range of users. It was developed for scientists seeking information and access to data pertaining to the Earth's land surface. GLIS contains references to regional, continental, and global data sets including land cover and land use, soils, topography, and data from aircraft and satellites. Direct access to GLIS is through wide-area networks and dial-up telecommunications interfaces:

Text terminal access:
telnet glis.cr.usgs.gov
Xwindows terminal access:
telnet xglis.cr.usgs.gov
PC access dial-up modem:
Contact GLIS user assistance to request PC dial-up GLIS software or download the software over Internet from sunl.cr.usgs.gov/pub/software/pcglis

GLIS User Assistance:

Telephone: 1-800-252-GLIS (1-800-252-4547)
FAX: 605-594-6589
E-mail: glis@glis.cr.usgs.gov

The Landsat images used in this booklet and their scene identification number and date of acquisition are listed below. The digital data are available on several types of media.

Description	Scene ID	Date
Glasgow, Missouri, USA	5025033009226810	September 24, 1992
	5025033009327010	September 27, 1993
Nile River Delta, Egypt	1190039007313090	May 10, 1973
	5177039008719990	July 18, 1987
Western Kansas, USA	1032034007222990	August 16, 1972
	5030034008822890	August 15, 1988

Description	Scene ID	Date
Northern Iran	2177035007719590	July 14, 1977
	5165035008725990	September 16,1987
Central Saudi Arabia	1180042007236090	December 25, 1972
	5167042008604690	February 15, 1986
Rondonia, Brazil	2249067007517090	June 19, 1975
	5232067008621390	August 1, 1986
	4232067009217410	June 22, 1992
Mount St. Helens, Washington, USA	1049028007325890	September 15,1973
	4046028008314290	May 22, 1983
	5046028008824490	August 31, 1988
Yellowstone Nat. Park, Wyoming, USA	5038029008820410	July 22, 1988
	4038029008827610	October 2, 1988
Kuwait	4165040009024310	August 31, 1990
	4165040009105410	February 23, 1991
	5165040009131810	November 14, 1991
Dallas-Fort Worth, Texas, USA	1029037007407190	March 12, 1974
	5027037008908190	March 22, 1989
South-Central Texas, USA	1029040007403590	February 4, 1974
	5027040008807990	March 19, 1988
Lake Chad, West Africa	1199051007234390	December 8, 1972
	5185051008728790	October 14, 1987
Aral Sea, Kazakhstan	1173028007314990	May 29, 1973
	5161028008723190	August 19, 1987
KBG, Caspian Sea, Turkmenistan	1177031007233990	December 4, 1972
	5164031008726890	September 25,1987
Lake Turkana, Kenya	1182057007303290	February 1, 1973
	4169057008901290	January 12, 1989
Great Salt Lake, Utah, USA	1042031007225790	September 13, 1972
	5039031008822790	August 14, 1988
Hubbard Glacier, Alaska, USA	5062018008521910	August 7, 1985
	5062018008625410	September 11,1986

References

Landsat

Holz, Robert, K., 1985, The Surveillant Science-Remote Sensing of the Environment, John Wiley and Sons Inc., New York, New York, 413 p.

Lillesand, Thomas, M., and Kiefer, Ralph, W., 1987, Remote Sensing and Image Interpretation, John Wiley and Sons Inc., New York, New York, 721 p.

Sabins, Floyd, F., 1987, Remote Sensing Principles and Interpretation, W. H. Freeman and Company, New York, New York, 449 p.

Short, N. M., Lowman Jr., P. D., Freden, S. C., and Finch Jr., W. A., 1976, Mission to Earth: Landsat views the world, National Aeronautics and Space Administration, NASA SP-360, Washington, D. C., 459 p.

U. S. Geological Survey, 1979, Landsat Data Users Handbook, 207 p.

U. S. Geological Survey, and National Oceanic and Atmospheric Administration, 1984, Landsat 4 Data Users Handbook, 244 p.

Agricultural Development

Nile River Delta, Egypt:

U. S. Bureau of the Census, 1994, Statistical Abstract of the United States: 1994, (114th Edition), Washington, D. C., 1011 p.

Theroux, Peter, and Reza, 1993, Cairo—clamorous heart of Egypt, National Geographic Magazine, vol. 183, no. 4, April, p. 38-68.

Helen Chapin Metz (ed.), 1991, Egypt: a country study, Federal Research Division, Library of Congress, Washington, D. C., 425 p.

Fox, Robert W., and Carroll, Allen, 1984, The urban explosion, National Geographic Magazine, vol. 166, no. 2, August, p. 179-185.

Abercrombie, Thomas J., 1977, Egypt: change comes to a changeless land, National Geographic Magazine, vol. 151, no. 3, March, p. 312-343.

Ellis, William, S., and Parks, Winfield, 1972, Cairo, Troubled Capital of the Arab World, National Geographic Magazine, vol. 141, no. 5, May, p. 639-667.

Western Kansas, USA:

Zwingle, Erla, and Richardson, Jim, 1993, Ogallala aquifer: wellspring of the high plains, National Geographic Magazine, vol. 183, no. 3, March, p. 80-109.

Billard, Jules B., and Blair, James, P., 1970, The revolution in American agriculture, National Geographic Magazine, vol. 137, no. 2, February, p. 147-185.

Northern Iran:

Helen Chapin Metz (ed.), 1989, Iran: a country study, Federal Research Division, Library of Congress, Washington, D. C., 342 p.

Graves, William, and Blair, James, P., 1975, Iran: desert miracle, National Geographic Magazine, vol. 147, no. 1, January, p. 2-46.

Central Saudi Arabia:

Helen Chapin Metz (ed.), 1993, Saudi Arabia: a country study, Federal Research Division, Library of Congress, Washington, D. C., 351 p.

Vesilind, Priit J., and Kashi, Ed, 1993, The Middle East's water—critical resource, National Geographic Magazine, vol. 183, no. 5, May, p. 38-70.

Azzi, Robert, 1980, Saudi Arabia: the kingdom and its power, National Geographic Magazine, vol. 158, no. 3, September, p. 286-332.

Forest Change

Rondonia, Brazil:

Skole, David, and Tucker, Compton, 1993, Tropical Deforestation and Habitat Fragmentation in the Amazon: Satellite Data from 1978 to 1988, Science, American Association for the Advancement of Science, Washington, D. C., vol. 260, no. 5116, June, p. 1905-1910.

Ellis, William S., Allard, William, A., and McIntyre, Loren, 1988, Rondonia: Brazil's imperiled rain forest, National Geographic Magazine, vol. 174, no. 6, December, p. 772-799.

White, Peter T., and Blair, James, P., 1983, Tropical rain forests: Nature's dwindling treasures, National Geographic Magazine, vol. 163, no. 1, January, p. 2-46.

Natural Disaster

Mount St. Helens, Washington, USA:

Lipman, Peter, W., and Mullineaux, Donal, R., (ed.), 1981, The 1980 Eruptions of Mount St. Helens, Washington, U. S. Geological Survey Professional Paper 1250, Washington, D. C., 844 p.

Hays, W. W., (ed.), 1981, Facing Geologic and Hydrologic Hazards, Earth Science Considerations, U. S. Geological Survey Professional Paper 1240-B, Washington, D. C., 108 p.

Findley, Rowe, and Raymer, Steve, 1981, Mount St. Helens aftermath, National Geographic Magazine, vol. 160, no. 6, December, p. 713-733.

Decker, Robert, and Decker, Barbara, 1981, The Eruptions of Mount St. Helens, Scientific American, Scientific American, Inc., New York, New York, March, vol. 244, no. 3, p. 68-80.

Findley, Rowe, 1981, Mount St. Helens: Mountain With a Death Wish, National Geographic Magazine, vol. 159, no. 1, January, p. 3-33.

Upper Mississippi River Basin:

Kelmelis, John, A., et. al., 1994, Science for Floodplain Management into the 21st Century, preliminary report of the Scientific Assessment and Strategy Team, 272 p.

Yellowstone National Park, Wyoming, USA:

Schullery, Paul, 1989, The Fires and Fire Policy, Bioscience, American Institute of Biological Sciences, Washington, D. C., vol. 39, no. 10, November, p. 686-694.

Jeffery, David, 1989, Yellowstone: the Great Fires of 1988, National Geographic Magazine, vol. 175, no. 2, February, p. 255-273.

Williams, Ted, 1989, Incineration of Yellowstone, Audubon, National Audubon Society, New York, New York, vol. 91, no. 1, January, p. 38-85.

Kuwait:

Williams, Richard, S., Heckman, Joanne, and Schneeberger, J., 1991, Environmental Consequences of the Persian Gulf War 1990-1991 Remote Sensing Datasets of Kuwait and Environs, National Geographic Society, 48 p.

Urban Growth

Dallas-Fort Worth, Texas, USA:

U. S. Bureau of the Census, 1992, Population Trends in the 1980's, Current Population Reports, Special Studies Series P-23, no. 175, May, 63 p.

Smith, Griffin, and Harvey, David, A., 1984, Dallas!, National Geographic Magazine, vol. 166, no. 3, September, p. 272-305.

U. S. Bureau of the Census, 1980, Statistical Abstract of the United States: 1980, (101st Edition), Washington, D. C., 1059 p.

South-Central Texas, USA:

U. S. Bureau of the Census, 1994, Statistical Abstract of the United States: 1994, (114th Edition), Washington, D. C., 1011 p.

Moize, Elizabeth A., and O'Brien, Michael, 1990, Austin: deep in the heart of Texans: National Geographic Magazine, vol. 177, no. 6, June, p. 50-71.

U. S. Bureau of the Census, 1980, Statistical Abstract of the United States: 1980, (101st Edition), Washington, D. C., 1059 p.

Water Resources

Lake Chad, West Africa:

Hutchinson, Charles, F., Warshall, Peter, Arnould, Eric, J., and Kindler, Janusz, 1992, Development in Arid Lands: Lessons from Lake Chad, Environment, vol. 34, no. 6, July-August, p. 16-43.

Collelo, Thomas (ed.), 1990, Chad: a country study, Federal Research Division, Library of Congress, Washington, D. C., 252 p.

Ellis, William S., and McCurry, Steve, 1987, Africa's Stricken Sahel, National Geographic Magazine, vol. 172, no. 2, August, p. 140-179.

Schneider, Stanley, R., McGinnis, David, F., and Stephens, George, 1985, Monitoring Africa's Lake Chad basin with Landsat and NOAA satellite data, International Journal of Remote Sensing, vol. 6, no. 1, January, p. 59-73.

Aral Sea, Kazakhstan:

Perera, Judith, 1993, A sea turns to dust, New Scientist, New Scientist Publications, London, England, vol. 140, no. 1896, October 23, p. 24-27.

Micklin, Philip, P., 1992, The Aral Crisis: Introduction to the Special Issue, Post-Soviet Geography, V. H. Winston and Son, Inc., Silver Spring, Maryland, vol. 33, no. 5, May, p. 269-282.

Rich, Vera, 1991, A new life for the sea that died?, New Scientist, New Scientist Publications, London, England, vol. 130, no. 1763, April 13, p. 15.

Ellis, William S., and Turnley, David, C., 1990, A Soviet Sea Lies Dying, National Geographic Magazine, vol. 177, no. 2, February, p. 73-93.

New Scientist, 1989, Soviet cotton threatens a region's sea—and its children, New Scientist Publications, London, England, vol. 124, no. 1691, November 18, p. 22.

Perera, Judith, 1988, Where glasnost meets the greens, New Scientist, New Scientist Publications, London, England, vol. 120, no. 1633, October 8, p. 25-26.

Kara-Bogaz-Gol, Caspian Sea, Turkmenistan

Rodionov, S. N., 1990, A Climatological Analysis of the Unusual Recent Rise in the Level of the Caspian Sea, Soviet Geography, V. H. Winston and Son, Inc., Silver Spring, Maryland, vol. 31, no. 4, April, p. 265-275.

Leont'yev, O. K., 1988, Problems of the Level of the Caspian and the Stability of its Shoreline, Soviet Geography, V. H. Winston and Son, Inc., Silver Spring, Maryland, vol. 29, no. 6, June, p. 608-616.

Shabad, Theodore, 1985, Aqueduct Completed to Feed Caspian Water Into Dried-up Kara-Bogaz-Gol, Soviet Geography, V. H. Winston and Son, Inc., Silver Spring, Maryland, vol. 26, no. 1, January, p. 59-61.

New Scientist, 1988, The lingering death of the Caspian Sea, New Scientist Publications, London, England, vol. 118, no. 1611, May 5, p. 26.

Shabad, Theodore, 1980, Caspian Sea "Leak" is Stopped, Soviet Geography, V. H. Winston and Son, Inc., Silver Spring, Maryland, vol. 21, no. 5, May, p. 322-323.

Lake Turkana, Kenya:

Johnson, Thomas, C., Halfman, John, D., Rosendahl, Bruce, R., and Lister, Guy, S., 1987, Climatic and tectonic effects on sedimentation in a rift-valley lake: Evidence from high-resolution seismic profiles, Lake Turkana, Kenya, Geological Society of America Bulletin, Geological Society of America, Inc., Boulder, Colorado, vol. 98, no. 4, April, p. 439-447.

Cerling, Thure, E., 1986, A mass-balance approach to basin sedimentation: constraints on the recent history of the Turkana Basin, Palaeogeography, Palaeoclimatology, Palaeoecology, vol. 54, no. 1-4, May, p. 63-86.

Nelson, Harold, D., (ed.), 1984, Kenya: a country study, Federal Areas Studies, The American University, Washington, D. C., 334 p.

Yuretich, Richard, F., 1979, Modern sediments and sedimentary processes in Lake Rudolf (Lake Turkana) eastern Rift Valley, Kenya, Sedimentology, vol. 26, no. 3, June, p. 313-331.

Great Salt Lake, Utah, USA:

Gore, Rick, and Richardson, Jim, 1985, No way to run a desert, National Geographic Magazine, vol. 167, no. 6, June, p. 694-719.

Ware, Leslie, 1984, The Great Salt Lake gets greater every day, Audubon, National Audubon Society, New York, New York, vol. 86, no. 5, September, p. 118-131.

Hubbard Glacier, Alaska, USA:

Walker, K., M., and Zenone, C., 1988, Multitemporal Landsat Multispectral Scanner and Thematic Mapper Data of the Hubbard Glacier Region, Southeast Alaska, Photogrammetric Engineering and Remote Sensing, vol. 54, no. 3, March, p. 373-376.

Eliot, John, L., and Johns, Chris, 1987, Glaciers on the Move, National Geographic Magazine, vol. 171, no. 1, January, p. 106-119.

More image pairs are available in
"Earthshots: Satellite Images of Environmental Change,"
at
http://www.usgs.gov/Earthshots

ISBN 0-607-01000-2